CONTRACT SERIAL NO.
23440-9-9296-01-SS

CONTRACTOR: UNIVERSITY OF TORONTO

Final Report

on the

Physical Chemistry of Nickel Smelting

by

J.M. Toguri
Department of Metallurgy and Materials Science
University of Toronto
Toronto, Ontario
M5S 1A4

Submitted to: CANMET
Re: DSS Contract No. 064SS.23440-9-9296

75 pp

May 1992

MICROMEDIA

ABSTRACT

Cet article se rapporte à :

1)tension de surface et mesures de densité de Cu_2S,FeS et Ni_3S_2 et de leurs mélanges;

2)la saturation métallique dans le système Fe-Ni-Cu-S

3)le comportement mouillant du sulfure de Nickel

4)solubilité de l'oxygène dans le sulfure de Nickel.

La tension de surface et la densité du système ont été étudiées en fonction de la température et de la composition, en utilisant la technique de la pression maximum dans une bulle. Les résultats montrent que la densité de ces sulfures diminue quand la température augmente. La tension de surface de FeS augmente très légèrement quand la température augmente. A l'inverse la tension de surface de Ni_3S_2 décroit avec l'augmentation de température. La tension de surface de Cu_2S n'est pas dépendante de la température, dans la gamme de température étudée.

La tension de surface et la densité des systèmes Cu_2S-FeS, Cu_2S-Ni_3S_2, Ni_3S_2-FeS et Cu_2S-Ni_3S_2-FeS ont été mesurées à 1473 K. On a trouvé que FeS est un constituant qui active la surface dans tous les systèmes.

L'étude du diagramme de phase du système Fe-Ni-Cu-S a été menée. La limite de saturation du métal a été déterminée par la règle des segments inverses qui joignent le Nickel- Cuivre -Fer-sulfure de Nickel avec les phases alliées métalliques, dans une gamme de température comprise entre 1473 et 1673 K. Le rapport Nickel:Cuivre dans le sulfure de Nickel a varié de 3:1, 1:1, 1:3, tandis que le taux de Fe:Ni dans la phase alliée a varié de 10 à 90 en pourcentage massique de Ni.

La valeur initiale du taux de Ni:Cu n'affecte pas significativement la distribution de Nickel, Cuivre et Fer entre la phase alliée et la phase sulfurée.

La tension de surface et interfaciale du sulfure de Nickel est une propriété thermodymanique importante qui affecte des phénomènes comme la localisation de la corrosion sur les réfractaires, l'infiltration du sulfure de Nickel dans les réfractaires et l'infiltration de scories dans les métaux. Dans cette étude , la tension de surface de Ni-Fe-S a été mesurée en utilisant la technique de la goutte sur un substrat, disposée dans un appareillage haute -température équipé de radiographie X.

Pour obtenir les coordonnées nécessaires au calcul de la tension de surface, un programme informatique a été développé pour digitaliser le profil de la goutte. Cette nouvelle technique est fiable et rapide. Les résultats obtenus pour le système Ni-Fe-S, montrent qu'une augmentation de FeS conduit à une diminution de la tension de surface. Cette diminution est en désaccord avec les lois habituelles d'additivité.

La solubilité de l'oxygène dans les mélanges Ni-Fe-S-O a été déterminée dans les conditions suivantes: $10^{-11.5}<P_{O2}<10^{-8.5}$ atm; $0.19<Ni/(Ni+Fe)<0.85$, et 1473 K<T<1573 K. La solubilité de l'oxygène augmente avec la pression partielle de l'oxygène jusqu'à atteindre la valeur de saturation de l'oxyde. La présence de Fer facilite également la solubilité de l'oxygène. La dissolution de l'oxygène est inversement liée à PO2, et au taux Ni/(Ni+Fe); cependant, pour les valeurs élevées du rapport Ni/(Ni+Fe) (>0.5), la solubilité du sulfure apparait décroître en fonction du rapport Ni/(Ni+Fe), comme le fait également la solubilité de l'oxygène.

La valeur standart de l'énergie de Gibbs de la dissolution de l'oxygène dans Ni-Fe-S-O (pour Ni/(Ni+Fe)=0.47) peut être représentée dans la gamme de température 1473 K-1573 K par :

$$\Delta G^0 = -202.5 + 0.0660\ T\ (K)\ \ (+-1.5)\ KJ/mol$$

ABSTRACT

This report covers

1) surface tension and density measurements of Cu_2S, FeS, and Ni_3S_2 and its mixtures;

2) the metal saturation in the Fe-Ni-Cu-S system;

3) the wetting behavior of nickel mattes and;

4) oxygen solubilities in nickel mattes.

The surface tension and density of the Cu_2S, FeS, and Ni_3S_2 system was determined as a function of temperature and composition using the maximum bubble pressure technique. The density of these sulphides were found to decrease with increasing temperature. Surface tension measurements indicated that the values for FeS showed a slight increase with temperature. Ni_3S_2 showed a decrease in surface tension with increasing temperature. Cu_2S showed no dependency on temperature in the temperature range investigated.

Surface tension and density of the Cu_2S-FeS, Cu_2S-Ni_3S_2, Ni_3S_2-FeS and Cu_2S-Ni_3S_2-FeS systems were measured at 1473 K. It was found that FeS is a surface active component in all the systems.

The phase equilibria in the Fe-Ni-Cu-S system were investigated. The metal saturation boundary was identified by determining the tie lines which join the nickel-copper-iron mattes with the metallic alloy phase at temperatures between 1473 to 1673 K. The nickel:copper ratio in the matte phase was varied from 3:1, 1:1 and 1:3, while the Fe:Ni in the alloy phase was varied from 10 to 90 mass percent Ni.

The value of the input ratio of Ni:Cu does not significantly affect the distribution of nickel, copper and iron between the alloy phase and the sulphide phase.

Surface tension and interfacial tension of nickel matte is an important thermodynamic property which affects phenomena such as localized corrosion of refractories, infiltration of matte into refractories and entrainment of pay metal into slags. In this study, the surface tension of Ni-Fe-S matte was measured using the sessile drop technique together with a high temperature x-ray radiographic setup.

To obtain the profile coordinates required for surface tension calculation, a computer program was developed to digitize the drop profiles. This new digitization technique was found to be reliable and less time consuming. The surface tension data obtained for the Ni-Fe-s system showed an increase in FeS content in the matte corresponds to a decrease in surface tension. This decrease showed a negative deviation from the ideal rule of additivity.

Oxygen solubilities were determined in Ni-Fe-S-O melts under the following conditions: $10^{-11.5} \leq Po_2 \leq 10^{-8.5}$ atm; $0.19 \leq Ni/(Ni+Fe) \leq 0.85$; and $1473\ K \leq T \leq 1573\ K$. The oxygen solubility was found to increase with the partial pressure of oxygen up to a maximum value at oxide saturation. The ferrous metal content enhanced oxygen solubility. Oxygen dissolution behavior was inversely related with respect to Po_2, and the Ni/(Ni+Fe) ratio; however, at high matte grade {Ni/(Ni+Fe) > ~0.5}, sulphur solubility appeared to decrease as a function of the Ni/(Ni+Fe) ratio, as did oxygen solubility.

The standard Gibbs energy of oxygen dissolution in Ni-Fe-S-O melts {Ni/(Ni+Fe) = 0.47} can be represented, in the temperature range, 1473 to 1573 K, by

$$\Delta G^0 = -202.5 + 0.0660\ T\ (K) \quad (\pm 1.5)\ KJ/mol$$

Part I

The Surface Tension and Density of Cu_2S, FeS, Ni_3S_2 and Its Mixtures

Abstract

The surface tension and density of the Cu_2S, FeS and Ni_3S_2 system was determined as a function of temperature and composition using the maximum bubble pressure technique. The density of these sulphides were found to decrease with increasing temperature. Surface tension measurements indicated that the values for FeS showed a slight increase with temperature. Ni_3S_2 showed a decrease in surface tension with increasing temperature. Cu_2S showed no dependency on temperature at the temperature range investigated.

Surface tension and density of the Cu_2S-FeS, Cu_2S-Ni_3S_2, Ni_3S_2-FeS and Cu_2S-Ni_3S_2-FeS systems were measured at 1473 K. It was found that FeS is a surface active component in all the systems.

Introduction

Physical properties of liquid mattes plays an important role in the pyrometallurgy of copper and nickel [1, 2]. They can influence phenomena such as matte entrainment in slag and corrosion of refractory bricks. In order to fully understand and describe such phenomena, precise measurements of physical properties such as surface tension and density are required. Due to the experimental difficulties involved, both density and surface tension data for copper and nickel mattes are scarce and scattered. Therefore, the aim of this study is to determine accurately the surface tension and density of the copper and nickel matte system.

Experimental

The three different sulphides, Cu_2S, FeS, and Ni_3S_2, used in this study were prepared using high purity metals and sulphur. They were fused at high temperature under a hydrogen atmosphere. The final sulphur content in these 'master' samples were found to contain 20.6%, 37% and 26.7% for Cu_2S, FeS, and Ni_3S_2 respectively. When mixture of these sulphides was required, it was melted in the experimental furnace prior to the experiment.

The experimental technique used for obtaining both surface tension and density measurements was the maximum bubble pressure technique. In this technique, gas bubbles were allowed to form slowly at the tip of a capillary. The maximum pressure allowable inside the bubble is determined by the surface tension and the depth for which the capillary was immersed. To evaluate the surface tension, the method outlined by Sugden [3, 4] was used. And to determine the density of the melt by this technique, equation 1 was used. According to this equation, density is represented by the slope on a plot of the maximum pressure inside the gas bubble against immersion depth.

$$P(h) = \frac{2\gamma}{r} + \rho g h \qquad (1)$$

where

P = maximum bubble pressure;

h = depth of immersion;

γ = surface tension;

r = radius of capillary;

ρ = density and;

g = gravitational acceleration;

A schematic of the experimental setup is shown in Figure 1. The apparatus consists of a Glowbar furnace (1), a gas train (2), an alumina capillary tube (3), an alumina crucible for containing the melt (4), a pressure transducer (5) for measuring the gas pressure, and a motor drive mechanism (6) for raising and lowering the capillary to the precise depth. The gas bubbling rate in the melt was regulated by a gas overflow arrangement (9) and any pressure fluctuation inside the furnace was stabilized by a buffer vessel (8). Temperature of the sample was monitored by a Pt-Pt/13%Rh thermocouple (11). The sheath of the thermocouple also served as a support rod for the crucible.

To start an experiment, the sample was first placed at the cold zone of the

furnace and the reaction tube was sealed with the bottom end cap. Ultra high purity argon was used to purge the tube for 12 hours while the buffer vessel was closed off from the reaction tube. At the end of the purge, the furnace was brought up to experimental temperature and the sample was pushed up to the hot zone. After about one hour, the capillary was lowered into one of the three chosen depth (0.635, 1.270, and 1.905 cm) of the melt. The path to the buffer vessel was opened before gas bubbling began. Ultra high purity argon was used as the bubbling gas and the bubbling frequency used was in the range of 30-60 seconds per bubble. Ten to 15 pressure measurements were obtained for each immersion depth.

Results and Discussion

The surface tension and density for Cu_2S, FeS, and Ni_3S_2 were measured in the temperature range of 1273-1573 K. The results of these measurements are presented in Figures 2 and 3. Each point on the graphs represents average value of 3-4 independent measurements. In the case of the density, all the sulphides showed a decrease with increasing temperature. As indicated in Figure 2, density of these sulphides is a linear function of temperature. Regression analyses of the data give the following equations:

$$\rho_{Ni_3S_2} = 6.144 - 0.00066T(^oK) \quad g/cm^3 \tag{2}$$

$$\rho_{Cu_2S} = 6.075 - 0.00054T(^oK) \quad g/cm^3 \tag{3}$$

$$\rho_{FeS} = 5.435 - 0.0011T(^oK) \quad g/cm^3 \tag{4}$$

Density results obtained in this study are compared to the FeS and Cu_2S results obtained by Tokumoto et al [5] which were obtained by the sessile drop technique. The present results showed reasonable good agreement with their data although the sessile drop

technique is not a very accurate method for density measurements. When the density data of FeS is compared to those obtained by Kaiura and Toguri [6], there is a 4-5% difference between the two set of data. Considering the difficulties encountered in high temperature experiments, the observed difference is small.

The surface tension of Ni_3S_2 showed a decrease with increasing temperature. On the other hand, the results of FeS and Cu_2S showed no temperature dependency (see Figure 3). The present surface tension measurement of FeS compared well with Tokumoto et al's [5] data. However, the results of Cu_2S showed a deviation of approximately 10%. This difference may be due to composition variation between the two sets of data. It could also be attributed to the difference in techniques used in the two studies. Tokumoto et al used the Bashforth and Adams' table to evaluate surface tension. This is subjected to human bias since only three specific points were selected from the sessile drop for surface tension evaluation.

Surface tension and Density of the Cu_2S-FeS, Ni_3S_2-FeS and Cu_2S-Ni_3S_2 pseudo-binaries were measured at 1473 K. Surface tension data as a function of composition for the three systems are shown in Figures 4 to 6 respectively. Density results are shown in Figures 7 to 9.

The results of the Cu_2S-FeS system showed a non-linear relationship between surface tension and matte composition. The curvature of the regression line indicated that FeS is surface active in the system. When the present results are compared with literature data [5, 7] as illustrated in Figure 4, the surface tension obtained in this study showed lower values consistently. Such discrepancy may be attributed to composition difference and the experimental technique used to obtain the data. Nevertheless, all the results showed a similar dependency of surface tension on matte composition. Surface tension of the Ni_3S_2-FeS system (Figure 5) showed a less dramatic effect of FeS on surface tension. The relationship between surface tension and composition is almost linear. On the other hand, results obtained for the Cu_2S-Ni_3S_2 (Figure 6) system showed a similar trend to the one obtained for the Cu_2S-FeS system. In this case, Cu_2S acted as the surface active agent instead of FeS.

Density data for the Cu_2S-FeS system is shown in Figure 7, when combined with literature data [5, 6, 8], density showed a linear dependency on matte composition. The relationship between composition and density for this system can be expressed by equation 5. The correlation coefficient for the regression is 0.966.

$$\rho_{Cu_2S-FeS} = 3.897 + 1.2655X_{Ni_3S_2} \quad (5)$$

Density-composition relationship of the Ni_3S_2-FeS system is significantly different. As shown in Figure 8, density of the matte remained relatively constant over a large composition range for high grade matte. The density decreases only when mol fraction of Ni_3S_2 drops below about 0.5. Figure 9 shows the density for the Cu_2S-Ni_3S_2 system. The results indicated that density is again a linear function matte composition. The relationship can be expressed by equation 6.

$$\rho_{Cu_2S-Ni_3S_2} = 5.260 - 0.0955X_{Ni_3S_2} \quad (6)$$

Surface tension and density data for the Cu_2S-Ni_3S_2-FeS system are presented in Figures 10 and 11 respectively. As shown in Figure 10, surface tension of the matte is quite sensitive to composition changes (particularly with changes in fraction of Ni_3S_2 in the system) at the Ni_3S_2 corner. The results also indicated that addition of Cu_2S does not affect the surface tension significantly. This is indicated by the direction of the iso-tension lines which are pointing towards the Cu_2S corner. Density of the system exhibited a similar behavior. As illustrated in Figure 11, addition of Cu_2S has a very weak effect on the density of the matte. As for FeS, its behavior in the pseudo-ternary is very similar to that observed in the Ni_3S_2-FeS system.

Conclusions

Surface tension and density of Cu_2S, FeS and Ni_3S_2 and their mixtures have been measured using the maximum bubble pressure technique. It was found that for the pure sulphides, both the surface tension and density are linear function of temperature. For the psuedo-binaries, FeS and Cu_2S acted as surface active agent in the system. For the pseudo-ternary of Cu_2S-Ni_3S_2-FeS, both surface tension and density are not strongly influenced by the addition of Cu_2S to the system.

References

1. T. Nakamura and J.M. Toguri, in *Proc. Copper '91 - Pyrometallurgy of Copper*, C.Diaz, C. Landolt, A. Luraschi and C.J. Newman, Editor, Pergamon, New York, 1991, 537-51

2. J.F. Elliott, *Trans. Instn. Min. Metall.*, 94, 1986, C171-8.

3. S. Sugden, *J. Chem. Soc.*, 121, 1922, 858-66.

4. S. Sugden, *J. Chem. Soc.*, 125, 1924, 27-31.

5. S. Tokumoto, A. Kasama, and Y. Fujioka, *Technol. Report Osaka Univ.*, 22, 1972, 453-63.

6. G.H. Kaiura and J.M. Toguri, *Can. Metall. Quart.*, 18, 1979, 155-64

7. A.V. Vanyukov and V. Ya. Zaitsev, *Slags and Mattes in Non-Ferrous Metallurgy*, Moscow, 1969, p95

8. M. Nagamori, *Trans. AIME*, 245, 1969, 1897-

List of Figures

Figure 1. Experimental Apparatus.

Figure 2. Density of pure sulphides as a function of temperature.

Figure 3. Effect of temperature on the surface tension of some pure sulphides.

Figure 4. Surface tension isotherm of the Cu_2S-FeS system at 1473 K.

Figure 5. Surface tension isotherm of the Ni_3S_2-FeS system at 1473 K.

Figure 6. Surface tension isotherm of the Ni_3S_2-Cu_2S system at 1473 K.

Figure 7. Density isotherm of the Cu_2S-FeS system at 1473 K.

Figure 8. Density isotherm of the Ni_3S_2-FeS system at 1473 K.

Figure 9. Density isotherm of the Ni_3S_2-Cu_2S system at 1473 K.

Figure 10. Ternary surface tension diagram for the Ni_3S_2-Cu_2S-FeS system at 1473 K.

Figure 11. Ternary density diagram for the Ni_3S_2-Cu_2S-FeS system at 1473 K.

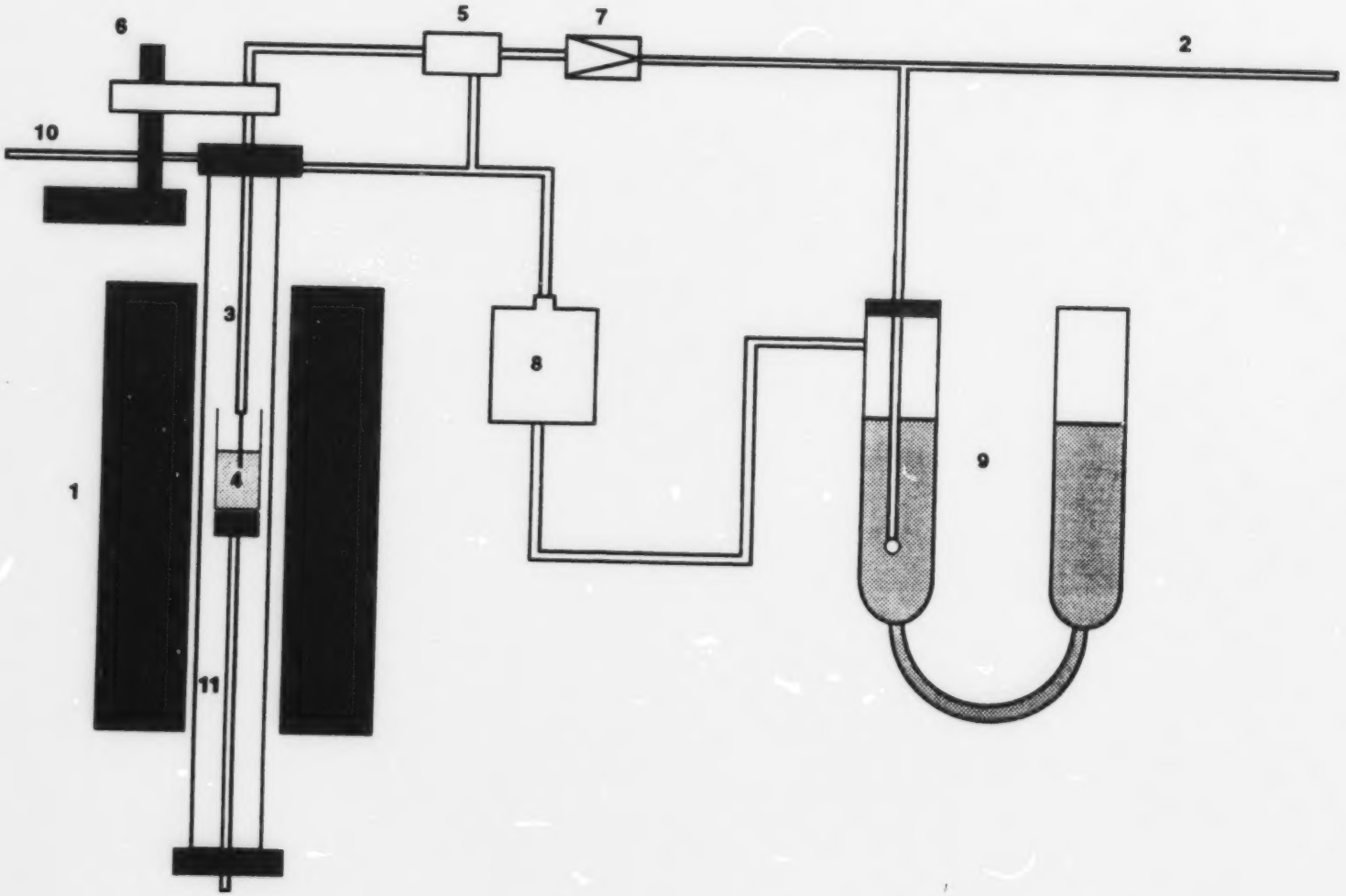

Fig 1

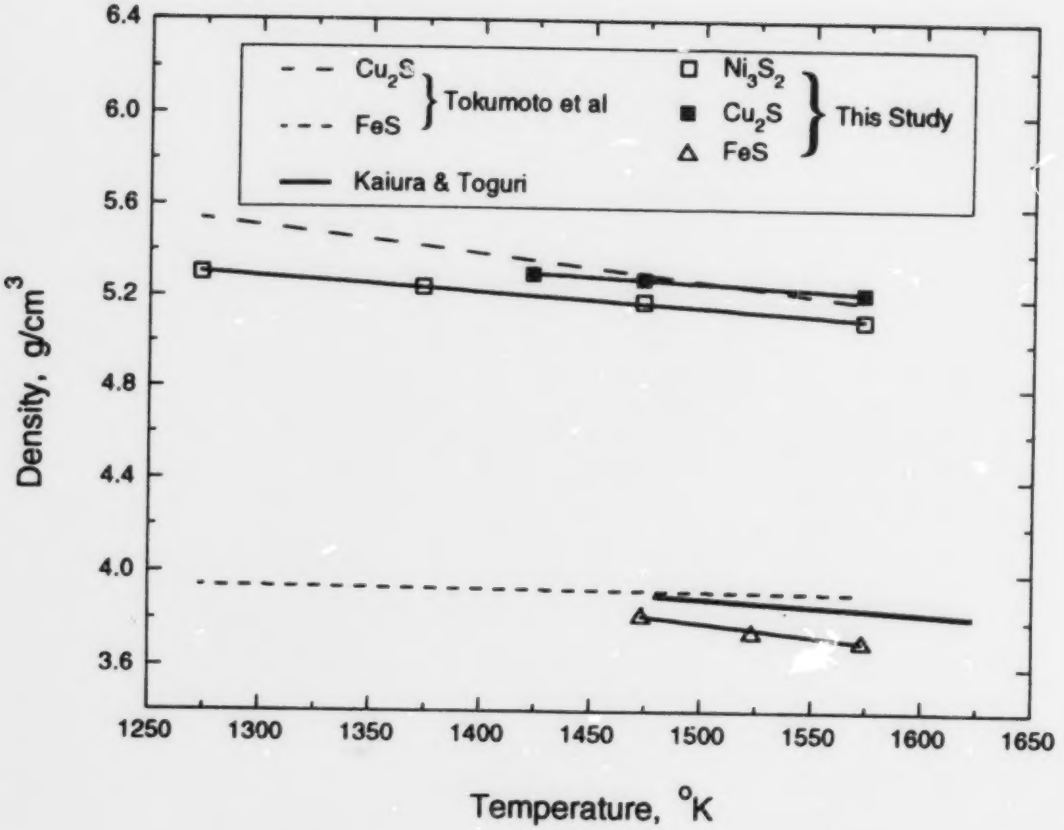
6.4
6.0
5.6
5.2
4.8
4.4
4.0
3.6
Density, g/cm3
1250
1300
1350
1400
1450
1500
1550
1600
1650
Temperature, °K
Cu2S
FeS
Tokumoto et al
Kaiura & Toguri
Ni3S2
Cu2S
FeS
This Study

Fig 2

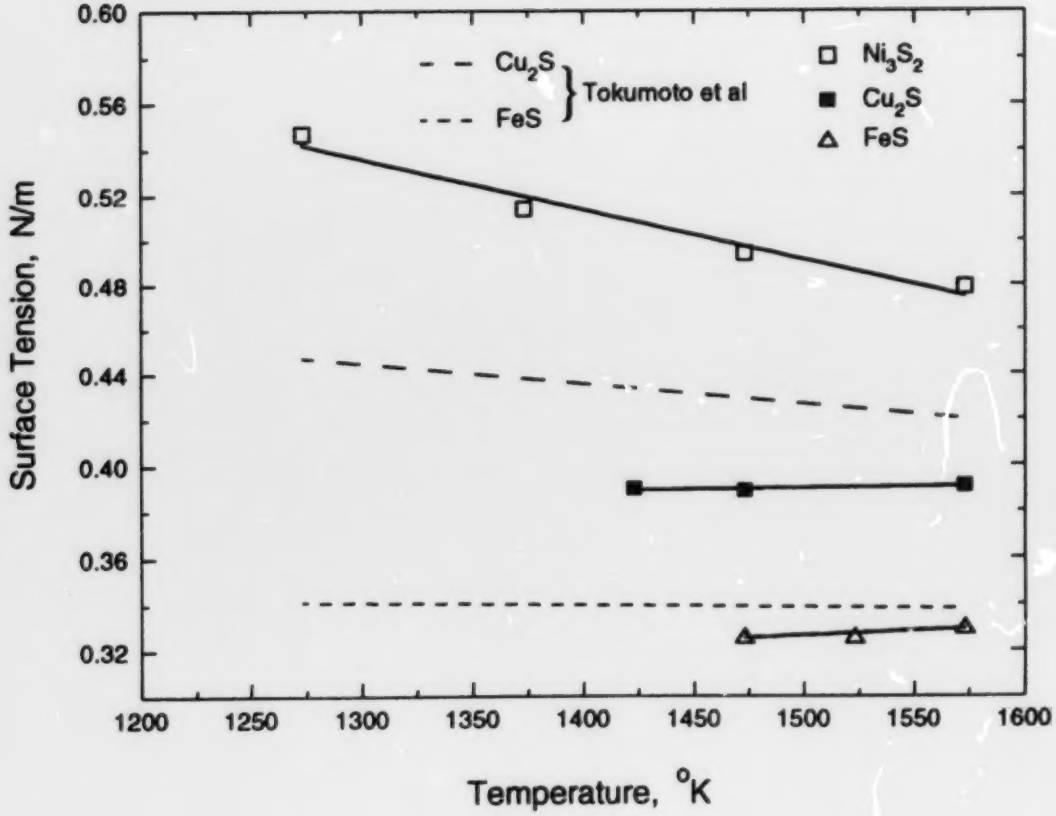
0.60
0.56
0.52
0.48
0.44
0.40
0.36
0.32
Surface Tension, N/m
1200
1250
1300
1350
1400
1450
1500
1550
1600
Temperature, °K
Cu2S
FeS
Tokumoto et al
Ni3S2
Cu2S
FeS

Fig 3

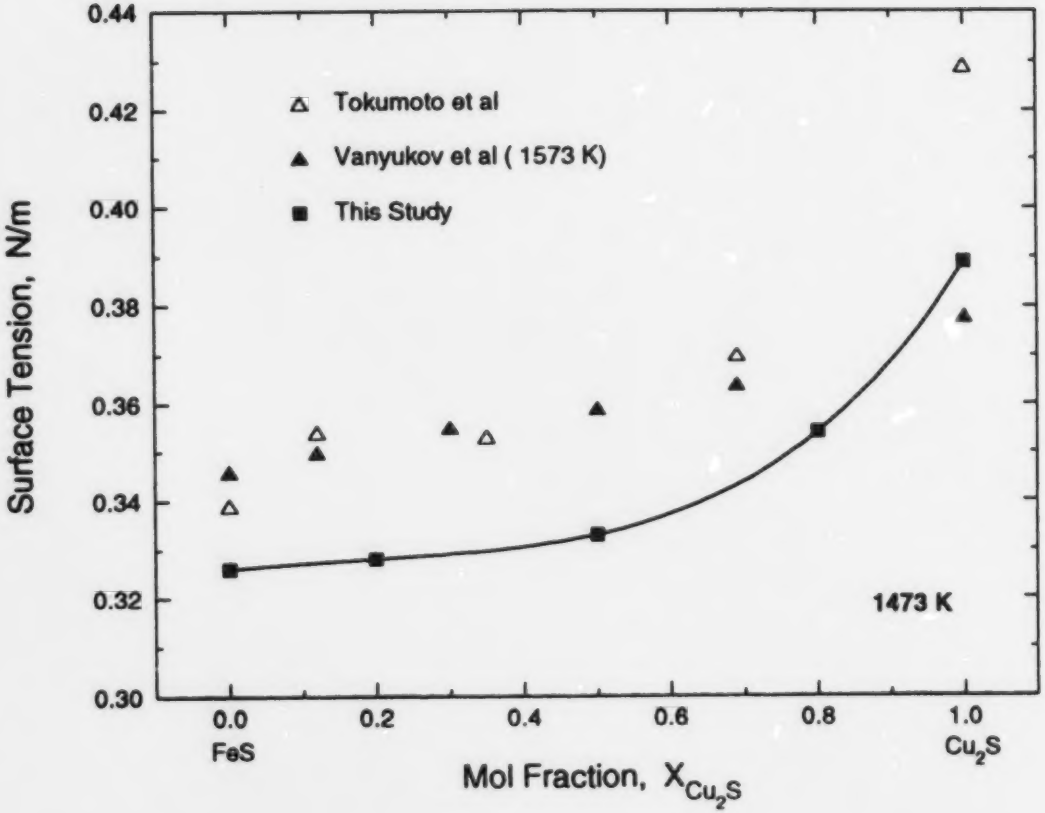
Surface Tension, N/m
0.44
0.42
0.40
0.38
0.36
0.34
0.32
0.30
Tokumoto et al
Vanyukov et al (1573 K)
This Study
1473 K
0.0
FeS
0.2
0.4
0.6
0.8
1.0
Cu2S
Mol Fraction, XCu2S

Fig 4

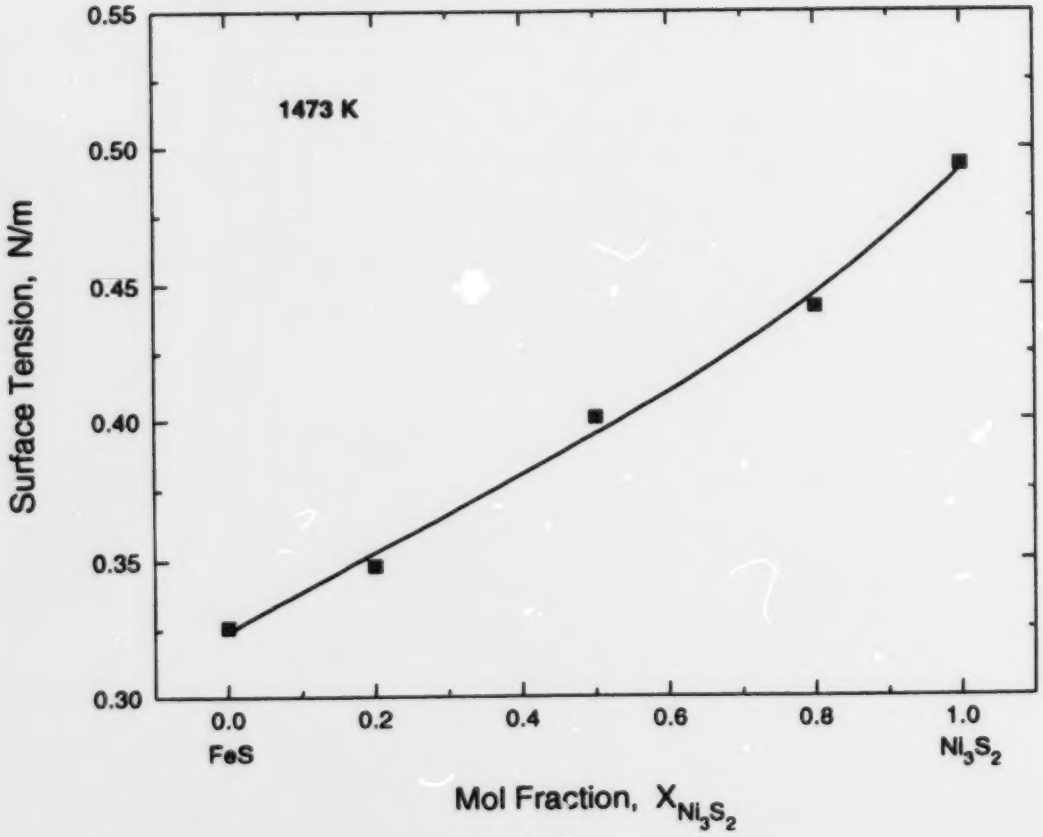
1473 K
Surface Tension, N/m
0.55
0.50
0.45
0.40
0.35
0.30
0.0
FeS
0.2
0.4
0.6
0.8
1.0
Ni_3S_2
Mol Fraction, $X_{Ni_3S_2}$

Fig 5

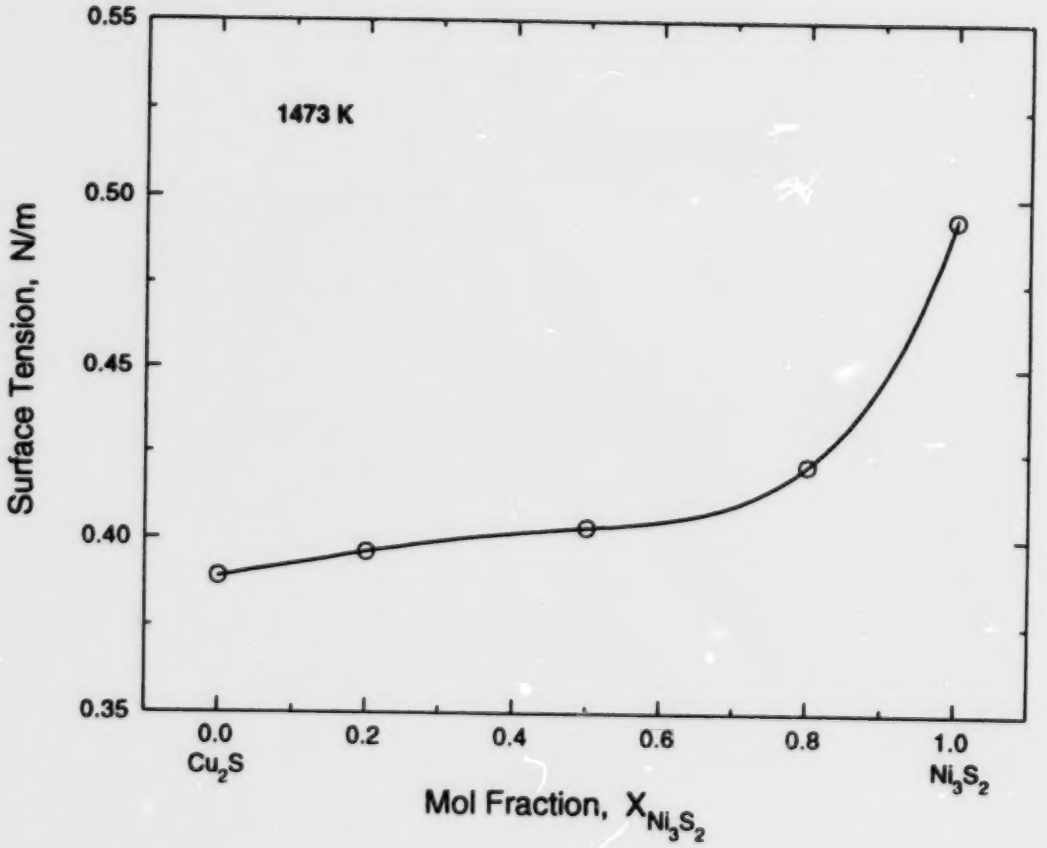
1473 K
Surface Tension, N/m
0.55
0.50
0.45
0.40
0.35
0.0
Cu2S
0.2
0.4
0.6
0.8
1.0
Ni3S2
Mol Fraction, XNi3S2

Fig 6

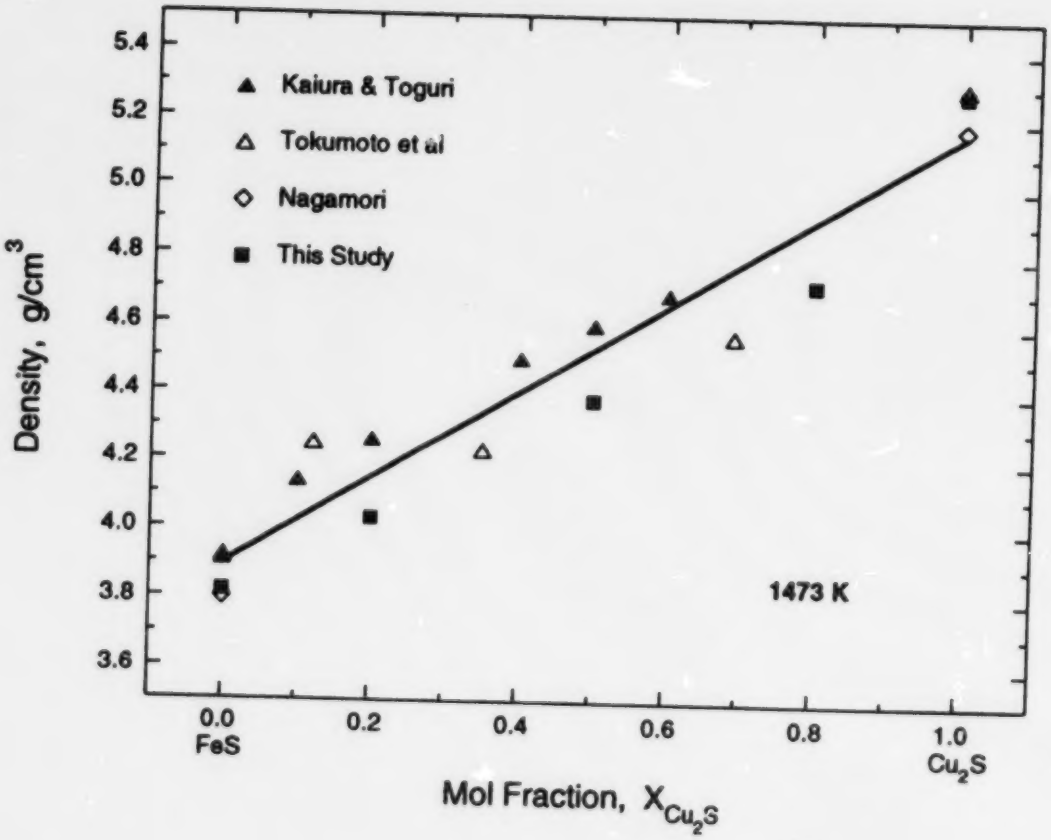
Density, g/cm^3
5.4
5.2
5.0
4.8
4.6
4.4
4.2
4.0
3.8
3.6
Kaiura & Toguri
Tokumoto et al
Nagamori
This Study
1473 K
0.0
FeS
0.2
0.4
0.6
0.8
1.0
Cu_2S
Mol Fraction, X_{Cu_2S}

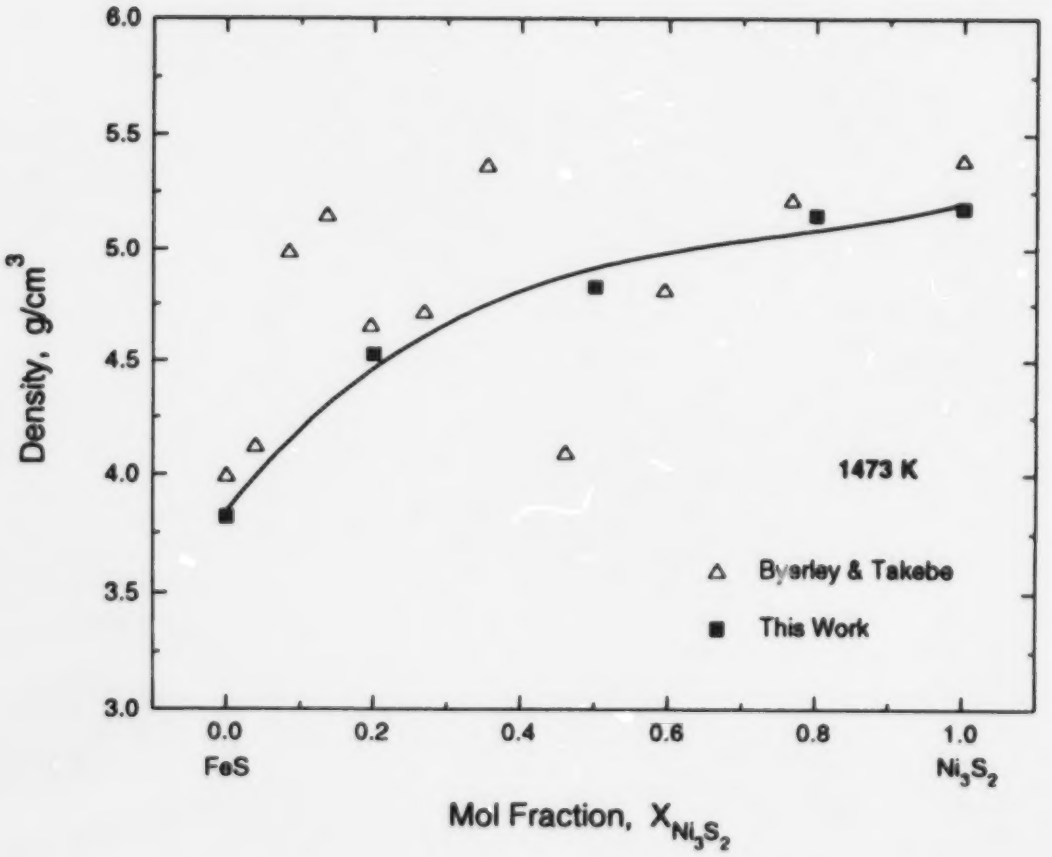
6.0
5.5
5.0
4.5
4.0
3.5
3.0
Density, g/cm^3
0.0
FeS
0.2
0.4
0.6
0.8
1.0
Ni_3S_2
Mol Fraction, $X_{Ni_3S_2}$
1473 K
Byerley & Takebe
This Work

Fig 8

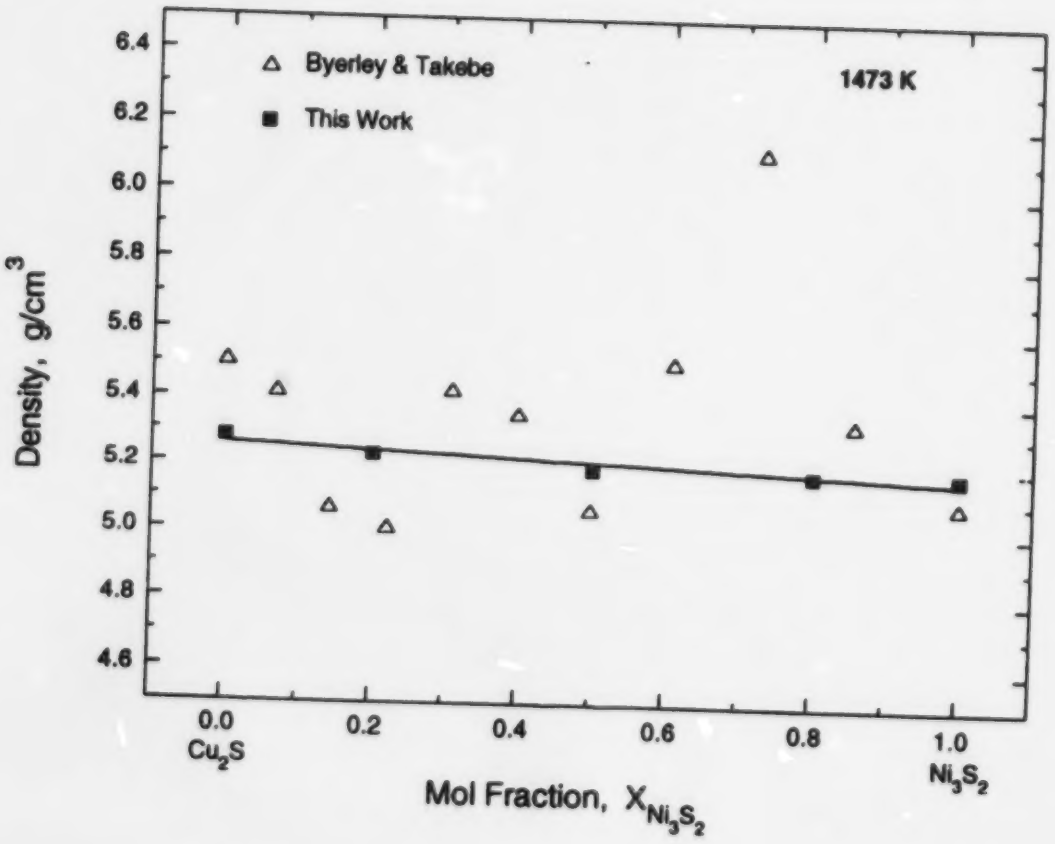
Byerley & Takebe
This Work
1473 K
Density, g/cm3
6.4
6.2
6.0
5.8
5.6
5.4
5.2
5.0
4.8
4.6
0.0
Cu2S
0.2
0.4
0.6
0.8
1.0
Ni3S2
Mol Fraction, XNi3S2

Fig 7

Fig 10

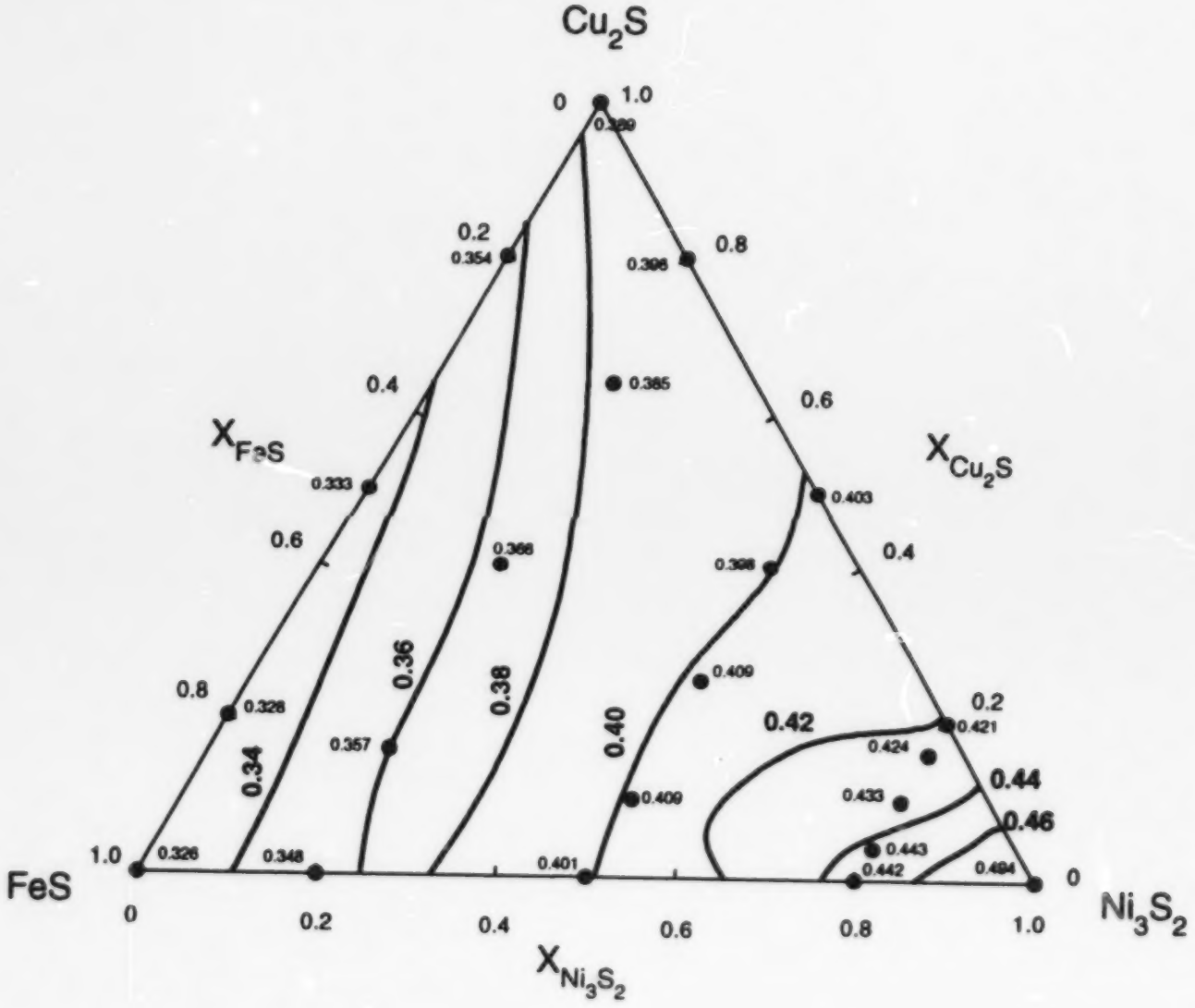
Cu2S
0
1.0
0.389
0.2
0.354
0.8
0.398
0.4
0.385
0.6
XFeS
XCu2S
0.333
0.403
0.6
0.366
0.4
0.398
0.8
0.328
0.36
0.38
0.409
0.2
0.34
0.357
0.42
0.421
0.424
0.40
0.44
0.409
0.433
0.46
1.0
0.326
0.348
0.401
0.443
0.442
0.494
0
FeS
0
0.2
0.4
0.6
0.8
1.0
Ni3S2
XNi3S2

Fig 11

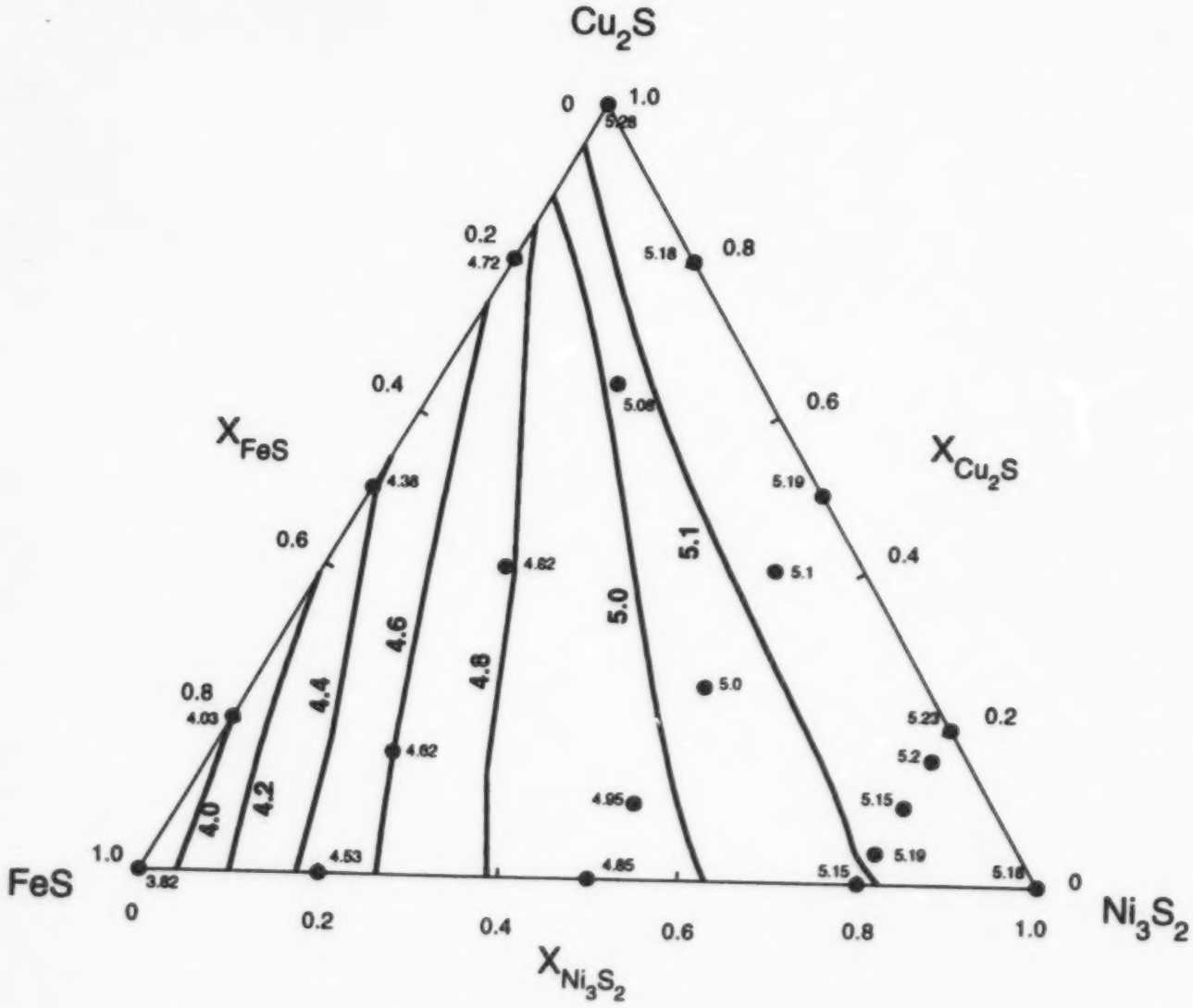
Cu2S
FeS
Ni3S2
XFeS
XCu2S
XNi3S2
0
0.2
0.4
0.6
0.8
1.0
5.28
5.18
4.72
5.08
4.38
5.19
4.82
5.1
5.0
4.03
5.23
4.62
5.2
4.95
5.15
5.19
3.82
4.53
4.85
5.15
5.16
4.0
4.2
4.4
4.6
4.8
5.0
5.1

Part II

Metal Saturation in the Fe-Ni-Cu-S System

ABSTRACT

The phase equilibria in the Fe-Ni-Cu-S system were investigated. The metal saturation boundary was identified by determining the tie lines which join the nickel-copper-iron mattes with the metallic alloy phase at temperatures between 1473 to 1673 K. The nickel:copper ratio in the matte phase was varied from 3:1, 1:1 and 1:3, while the Fe:Ni in the alloy phase was varied from 10 to 90 mass percent Ni.

The value of the input ratio of nickel:copper does not significantly affect the distribution of nickel, copper and iron between the alloy phase and the sulphide phase.

INTRODUCTION

When nickel-copper concentrates are subjected to a roast operation, iron sulphide and a small amount of nickel sulphides are oxidized. In order to recover the oxidized nickel, a reductive smelting operation is performed. During this procedure, and in the presence of sulphur deficiency, a metallic phase can result.

The purpose of this study is to identify the metal saturation boundary as a function of temperature and composition.

EXPERIMENTAL

The general procedure adopted for this study involved the equilibration of Fe-Ni alloys with Fe-Ni-Cu-S mattes in either quartz or alumina crucibles at the required temperature for a period of time under an argon atmosphere. Samples of the sulphide phase were taken by suction into a quartz tube which was then quenched. The metal phase was sampled by cooling the crucible that contained the original melt. Microscopic examinations were carried out to insure that the matte sample was free of primary metallics prior to chemical analysis. The primary metal phase in the crucible was analyzed by use of the scanning electron microscope (SEM).

A. Sample Preparation

The metals used for this study were electrolytic grade nickel, electrolytic grade copper, reagent grade iron and vacuum sublimated sulphur. Prior to use, the metals were all hydrogen reduced at 773 K to eliminate oxygen.

The iron-nickel alloys were prepared by melting the required iron and nickel in an induction furnace under a nitrogen atmosphere. The composition of these alloys is shown in Table 1.

Copper sulphide, nickel sulphide and iron sulphide were prepared by vacuum sealing the required amounts of respective metal and sulphur in quartz ampoules. The sealed ampoules were heated to 723 K for 72 h to allow the sulphur gas to react with the metal phase. Once the sulphur had reacted, the ampoules were heated to approximately 1473 K to melt and homogenize the sulphide, after which the samples were cooled.

The metal saturation line for the Fe-Ni-S system has been determined over the temperature 1473-1673 K by Lenz et.al. [1]. Using this work as the basis, the metal saturation boundary was evaluated with the addition of copper sulphide to the matte phase. Metal in the range 9 to 15 g, depending on the temperature and matte grade, were equilibrated with matte in the range 11 to 5 g.

B. Apparatus

The apparatus used for this study is shown in Fig. 1. It consists of a molybdenum furnace with a mullite reaction tube into which the sample containing the matte and alloy phase was placed. Argon was passed over a copper getter furnace (723 K) to remove oxygen, then passed into the reaction tube.

To obtain samples of matte, a 5 mm diameter quartz tube was used.

C. Equilibration Time

The time required to equilibrate the matte and metal phase was determined by keeping samples of identical chemical composition during 24, 48, 72 and 96 h at 1473 K. These samples were rapidly cooled, microscopically observed and analyzed for nickel and sulphur in the sulphide and metal phase. After 48 h, the upper sulphide and bottom metallic portion of the sample did not show change in composition, as shown in Fig. 2. From these series of experiments, 48 h was selected as the "equilibrium time".

At 1673 the equilibrium time was estimated as 32 h.

D. Chemical Analysis

The matte samples were examined optically, to insure that it was free of the primary metallic phase. The samples which were free of primary metallics, were analyzed chemically by Falconbridge Ltd. The metallic samples were analyzed by SEM using five iron-nickel standards. A typical trace showing the Fe, Ni, Cu and S content every 3 um along a line joining the centre of two metallic grains is illustrated in Fig. 3.

E. Experimental Procedure

The experimental procedure involved the following steps:

1. keeping the sample at the bottom of the furnace for 2 h to flush out any air introduced during the charging step,

2. slowly raising of the sample to the test temperature (45 min),
3. keeping the sample at the test temperature for about 1 h,
4. raising the temperature by 122 K to dissolve, during 30 min, the metal phase,
5. decreasing the temperature to the test temperature,
6. keeping the sample at the test temperature for about 46.5 h,
7. sampling of matte and
8. slowly cooling the remaining sample to avoid breaking of the sample holder tube.

RESULTS AND DISCUSSION

The chemical analysis for the equilibrated metal-sulphide phases (represented by the letters M and S, respectively) are given in Table 2 for the tests at 1473 K, in Table 3 for 1573 K and in Table 4 for 1673 K.

The results are also plotted on a ternary diagram where the corners represent Fe, Ni+Cu and S. The results for 1473, 1573 and 1673 K are shown in Figures 4, 5 and 6 respectively. The tie lines are indicated by a join between the two conjugate solutions. For comparison, the data reported by Lenz et.al. [1] for the Fe-Ni-S system, denoted by dashed line, and by Falconbridge [2] for the Fe-Ni-Cu-S system, denoted by full line, are shown.

For all the temperatures investigated Lenz et. al.'s results show lower sulphur contents, specially below 50% Ni+Cu, than those found in the present study. However, those reported by Falconbridge are significantly higher that those corresponding to this study, the higher the temperature is.

In Figure 7, the Ni+Cu mass percent is plotted against mass per cent sulphur in the matte for the three temperatures investigated. The line represents the two phase equilibria between matte and the metallic phase. To the right of the line, the matte phase is stable while to the left of the line the alloy phase is stable with respect to the matte.

The higher the Ni+Cu, the less sulphur is required to stabilize the matte phase. Once the equilibrium liquidus line is reached a further decrease in sulphur content results in the precipitation of a metallic iron-nickel-copper alloy. The three temperatures considered show the same tendency in respect to this effect, i.e. a continuous increase in sulphur with decreasing Ni+Cu content in matte.

Evaluation of commercial mattes at 1573 K [3], represented by triangles in Figure 7, agree quite well with the present results. The location of the Ni+Cu and S content of these samples lay on the right side of the sulphide-metal equilibrium line and therefore they should correspond to a homogeneous sulphide phase, which in fact occurred.

Based on the data of Figure 7, the effect of temperature upon the dissolution of sulphur, for different Ni+Cu contents in matte, is shown in Figure 8. Similar curves to the ones shown can be worked out for any desired Ni+Cu content in matte at the temperatures investigated.

Given a specific Ni+Cu content in matte the lower the equilibrium temperature the higher the sulphur content in matte. For example for Ni+Cu = 50% at 1573 K the matte phase dissolves approximately 9% S, while decreasing the temperature to 1473 K results in an increase to 16.5% S.

At the lower matte grades, i.e. low Ni+Cu content, the matte consists mainly of iron sulphide therefore, the limiting sulphur content corresponds to that of the Fe-S system at the temperature considered. For example the line representing the data at 1673 K will intersect the sulphur axis at 7%, while that at 1473 K does at 27% S.

The tendency observed in these curves is a decrease in sulphur with increasing temperature and with increasing matte grade. At 1473 K significant changes in sulphur content with matte grade occur. However, as the equilibration temperature increases the change in sulphur is less significant, i.e. at 1673 K.

The present results, Figure 7, clearly indicate that the input Ni to Cu ratio does not significantly affect the equilibrium distribution of Ni and Cu in the conjugate solution. It would appear that the replacement of Ni for Cu in the matte phase is additive. The additivity is particularly noticeable at the higher temperature. Thus, the more important compositional parameter is the mass percent of Ni+Cu.

CONCLUSIONS

The metal saturation line in the Fe-Ni-Cu-S system has been determined at temperature of 1473 K, 1573 K and 1673 K. The input nickel to copper ratio in the matte phase does not significantly affect the equilibrium distribution of Ni and Cu in the conjugate phase.

Ni and Cu are similar in atomic size and consequently form a complete solid solution. The present work has indicated that the assumption of the additivity of Ni+Cu is a more important compositional parameter.

REFERENCES

1. J.G. Lenz, B.R. Conard, R. Sridhar and J.S. Warner: Met. Trans. 9B (1978), 459-462.
2. Hatch Associates Ltd.: Internal Report-Falconbridge 1988.
3. C.M. Acuna and J.M. Toguri: Metal Saturation Studies of Commercial Matte Samples from Falconbridge, Report-Falconbridge March 1991.

Table 1: Composition of Prepared Samples

	Mass percent, %			
	Fe	Ni	Cu	S
A) Sulphides:				
Iron sulphide	70.96	-----	-----	29.04
Nickel sulphide	-----	87.34	-----	12.66
Copper sulphide	-----	-----	79.73	20.27
B) Alloys:				
Iron-10% Ni	87.04	12.96	-----	-----
Iron-30% Ni	67.72	32.28	-----	-----
Iron-50% Ni	47.61	52.39	-----	-----
Iron-70% Ni	28.31	71.69	-----	-----
Iron-90% Ni	10.52	89.48	-----	-----

Table 2: Results of chemical analysis for samples with different nickel to copper ratios equilibrated at 1473 K.

Sample Number	Chemical Composition (Mass percent, %) As reported Ni	Cu	Fe	S	Normalized Ni	Cu	Fe	S
Ni : Cu = 1 : 3								
1S	4.05	5.06	61.9	26.0	4.17	5.22	63.81	26.80
1M					6.60	1.22	92.18	-----
2S	11.8	13.0	49.8	23.1	12.08	13.31	50.97	23.64
2M					21.69	3.94	74.37	-----
3S	24.1	19.4	34.0	19.6	24.82	19.98	35.02	20.18
3M					39.55	8.76	51.69	-----
4S	41.4	20.6	22.7	11.5	43.04	21.41	23.60	11.95
4M					54.54	12.86	32.60	-----
5S	70.0	16.3	6.3	9.6	68.49	15.95	6.17	9.39
5M					78.17	11.92	9.91	-----
Ni : Cu = 1 : 1								
1S	5.3	3.3	64.6	25.4	5.38	3.35	65.51	25.76
1M					8.33	0.84	90.83	-----
2S	15.5	8.75	51.1	22.5	15.84	8.94	52.22	23.00
2M					25.05	3.10	71.85	-----
3S	34.2	10.3	35.1	16.8	35.48	10.68	36.41	17.43
3M					47.40	5.34	47.26	-----
4S	44.6	16.7	22.2	12.0	46.70	17.48	23.25	12.57
4M					57.88	10.34	31.78	-----
5S	61.6	18.4	7.5	9.0	63.83	19.07	7.77	9.33
5M					74.64	13.53	11.83	-----
Ni : Cu = 3 : 1								
1S	6.7	1.7	64.6	24.5	6.87	1.74	66.26	25.13
1M					10.15	0.49	89.36	-----
2S	19.2	4.5	53.4	21.9	19.39	4.55	53.94	22.12
2M					28.67	1.57	69.76	-----
3S	37.9	5.14	36.1	16.9	39.46	5.35	37.59	17.60
3M					49.64	2.79	47.57	-----
4S	51.2	9.4	22.6	12.8	53.33	9.80	23.54	13.33
4M					63.95	5.70	30.35	-----
5S	66.6	10.7	7.6	10.1	70.11	11.26	8.00	10.63
5M					80.03	7.98	11.99	-----

Table 3: Results of chemical analysis for samples with different nickel to copper ratios equilibrated at 1573 K.

Sample Number	Chemical Composition (Mass percent, %) As reported Ni	Cu	Fe	S	Normalized Ni	Cu	Fe	S
Ni : Cu = 1 : 3								
1S	6.0	4.6	66.0	23.2	6.01	4.61	66.13	23.25
1M					7.93	0.99	91.08	-----
2S	19.0	9.0	55.0	17.1	18.98	8.99	54.95	17.08
2M					24.07	3.64	72.29	-----
3S	40.5	8.8	43.0	8.8	40.07	8.70	42.53	8.70
3M					44.51	5.11	50.38	-----
4S	56.8	12.5	26.8	6.4	55.41	12.20	26.15	6.24
4M					56.73	8.10	35.17	-----
5S	74.5	14.5	8.5	6.0	71.98	14.01	8.21	5.80
5M					78.15	11.16	10.69	-----
Ni : Cu = 1 : 1								
1S	7.1	28.5	66.8	22.8	7.14	2.86	67.10	22.90
1M					8.87	0.71	90.42	-----
2S	21.5	6.3	55.5	16.6	21.52	6.30	55.56	16.62
2M					25.57	2.72	71.71	-----
3S	42.8	6.3	42.0	9.05	42.74	6.28	41.94	9.04
3M					46.37	3.94	49.69	-----
4S	58.0	9.3	25.5	7.2	58.00	9.30	25.50	7.20
4M					62.77	6.04	31.19	-----
5S	73.5	12.5	8.3	5.7	73.50	12.50	8.30	5.70
5M					80.03	9.05	10.92	-----
Ni : Cu = 3 : 1								
1S	8.0	0.60	65.0	22.6	8.32	0.62	65.57	23.49
1M					10.49	0.54	88.97	-----
2S	24.8	3.05	55.5	15.6	25.06	3.08	56.09	15.77
2M					28.47	1.36	70.17	-----
3S	45.3	3.53	40.8	9.34	45.77	3.57	41.22	9.44
3M					49.16	2.06	48.78	-----
4S	62.8	5.55	24.8	7.5	62.39	5.50	24.64	7.45
4M					66.41	3.77	29.82	-----
5S	77.5	7.0	7.8	6.8	78.20	7.06	7.88	6.86
5M					84.57	4.96	10.47	-----

Table 4: Results of chemical analysis for samples with different nickel to copper ratios equilibrated at 1673 K.

Sample Number	Chemical Composition (Mass percent, %) As reported Ni	Cu	Fe	S	Normalized Ni	Cu	Fe	S
Ni : Cu = 1 : 3								
1S	12.0	1.19	81.6	4.75	12.06	1.19	81.98	4.77
1M					10.72	0.72	88.56	-----
2S	30.2	1.93	64.5	2.55	30.45	1.95	65.03	2.57
2M					28.73	1.29	69.98	-----
3S	49.5	1.60	44.8	1.68	50.73	1.64	45.91	1.72
3M					51.08	1.06	47.86	-----
4S	66.5	2.51	27.2	1.22	68.25	2.58	27.92	1.25
4M					69.60	1.70	28.70	-----
5S	84.5	3.15	9.0	1.39	86.19	3.21	9.18	1.42
5M					88.86	2.20	8.94	-----
Ni : Cu = 1 : 1								
1S	12.0	0.78	81.6	4.77	12.10	0.79	82.30	4.81
1M					11.35	0.62	88.03	-----
2S	29.8	1.26	66.2	2.65	29.83	1.26	66.26	2.65
2M					28.75	0.87	70.38	-----
3S	50.0	1.16	44.8	1.71	51.19	1.19	45.87	1.75
3M					51.15	0.77	48.08	-----
4S	68.5	1.27	27.0	1.07	70.01	1.30	27.60	1.09
4M					70.78	0.92	28.30	-----
5S	85.5	2.20	8.8	2.03	86.78	2.23	8.93	2.06
5M					89.28	1.60	9.12	-----
Ni : Cu = 3 : 1								
1S	12.9	0.42	82.1	4.15	12.96	0.42	82.45	4.17
1M					11.36	0.48	88.16	-----
2S	30.0	0.68	66.4	2.75	30.05	0.68	66.51	2.76
2M					29.49	0.64	69.87	-----
3S	50.5	0.61	44.8	1.40	51.90	0.62	46.04	1.44
3M					51.00	0.64	48.36	-----
4S	68.5	1.11	27.0	1.11	70.09	1.14	27.63	1.14
4M					71.07	0.71	28.22	-----
5S	86.5	1.24	9.0	1.49	88.06	1.26	9.16	1.52
5M					89.78	1.05	9.17	-----

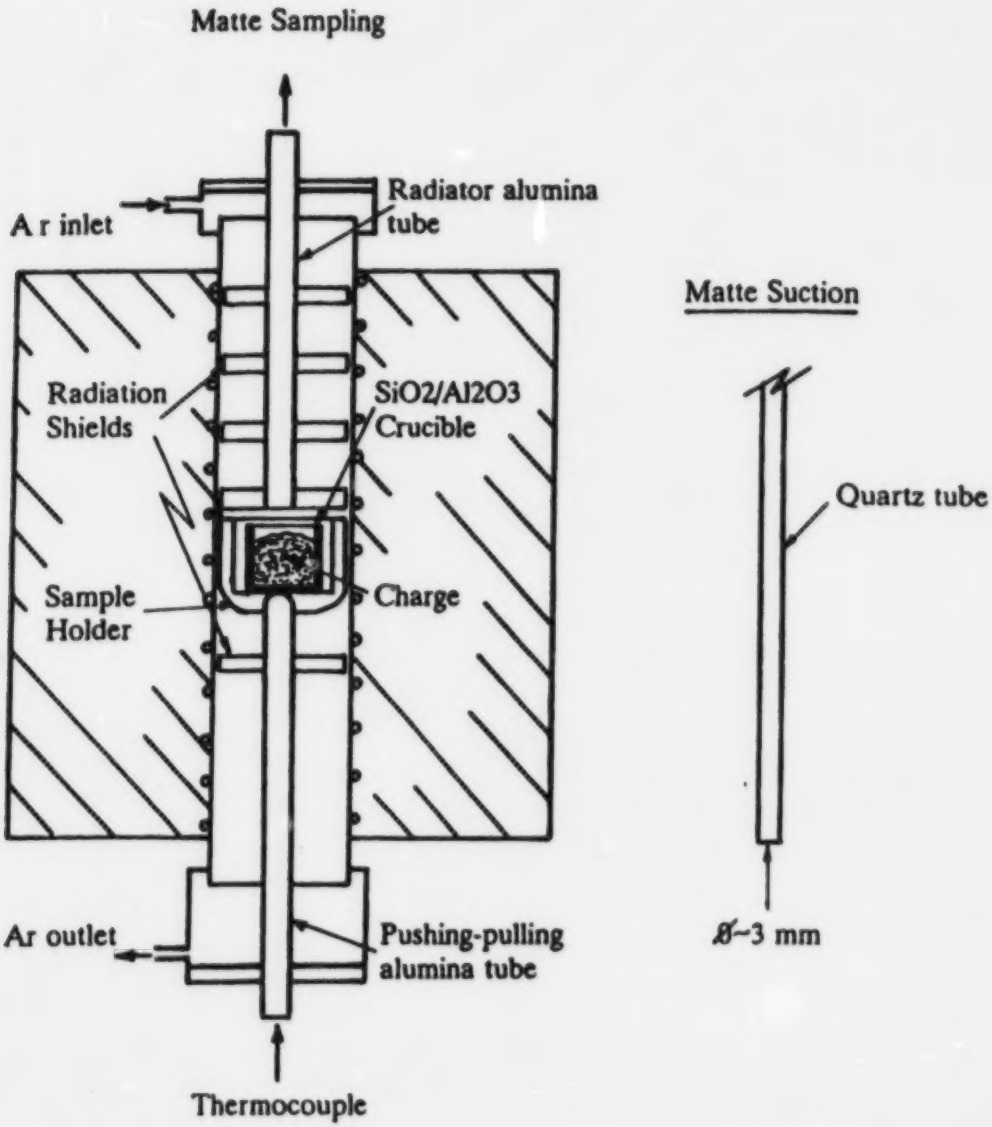

Figure 1: Schematic representation of the furnace set up.

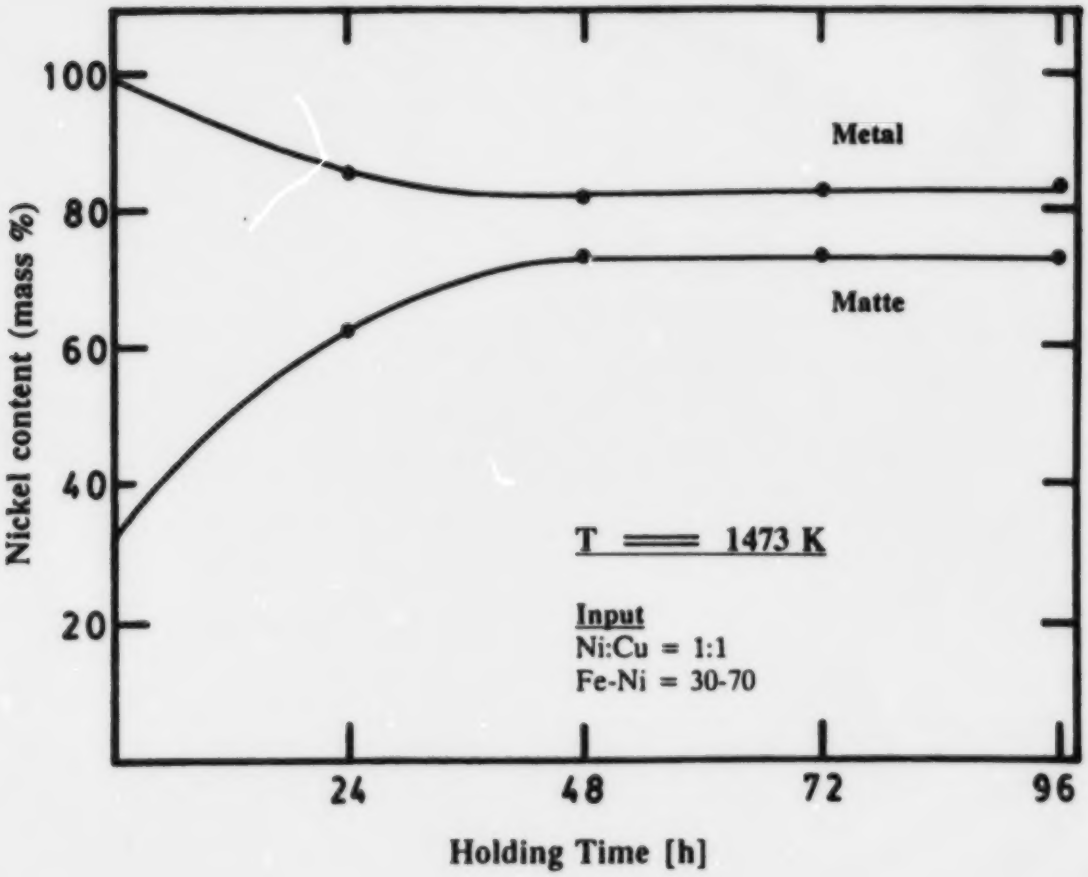

Figure 2: Determination of the "equilibrium time". It corresponds to the time where the plateau for nickel content in matte and metal is reached

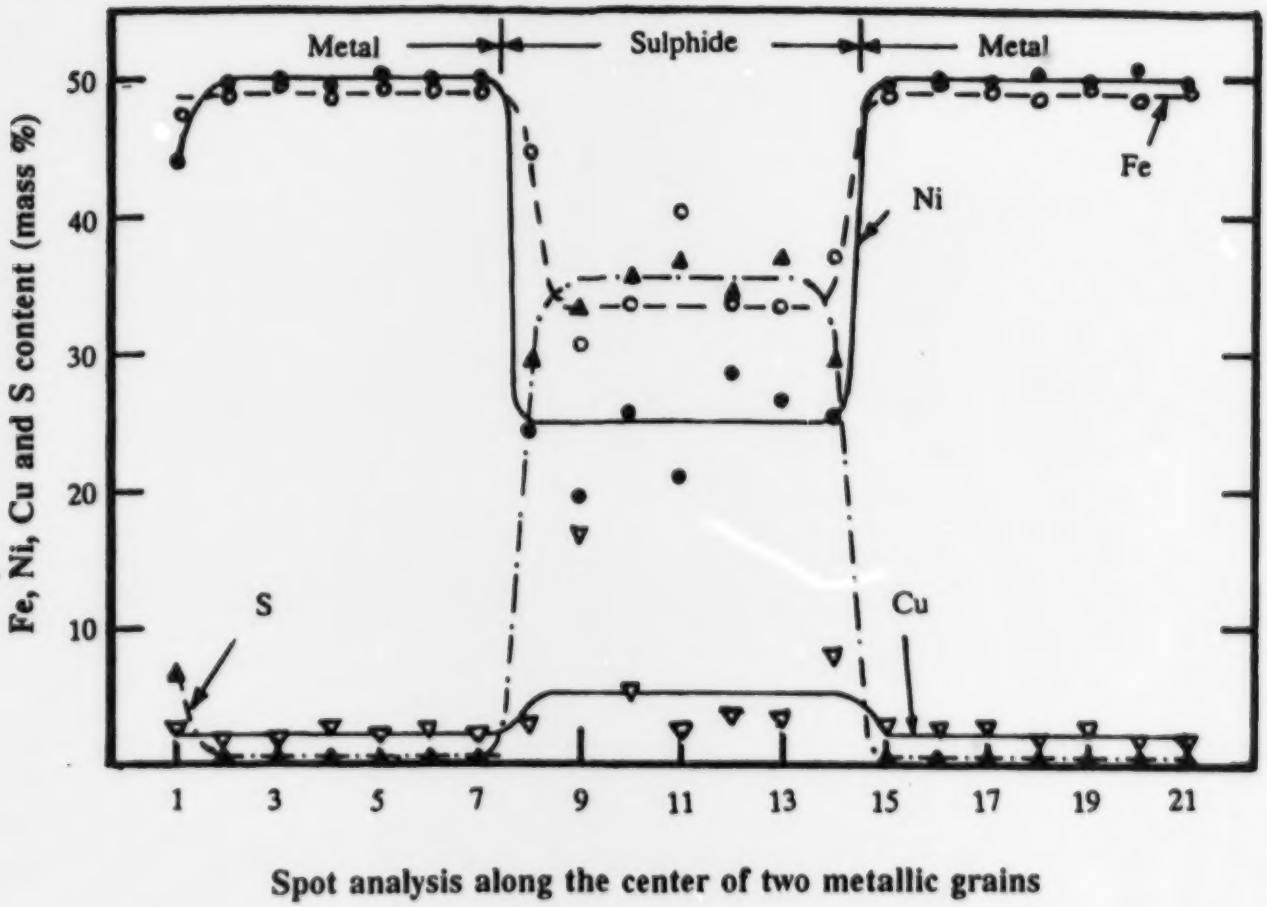

Figure 3: Gradient concentration along the line joining the centre of two metallic grains.

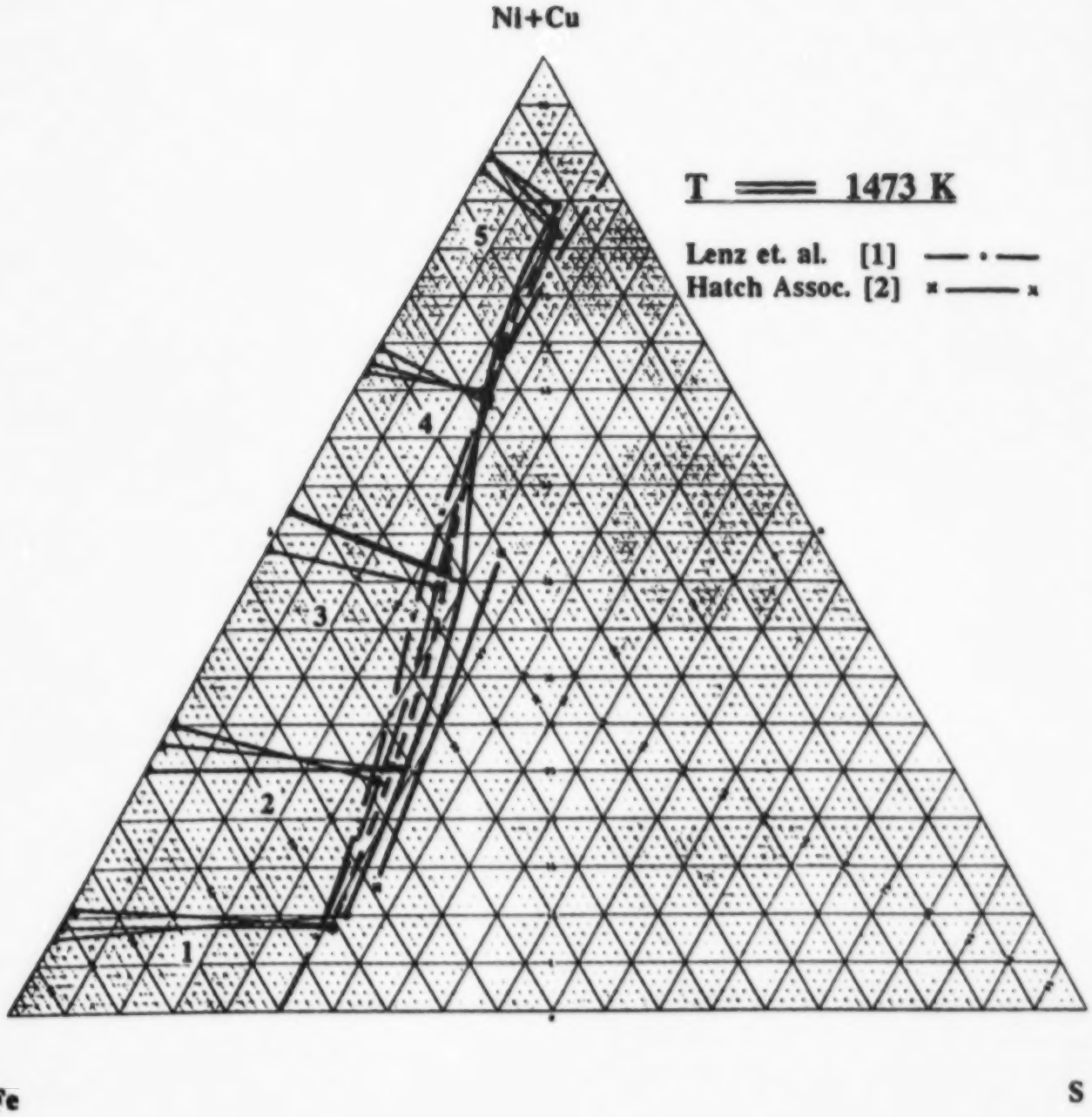

Figure 4: Representation of experimental results on a Fe-Ni+Cu-S pseudoternary system at 1473 K.

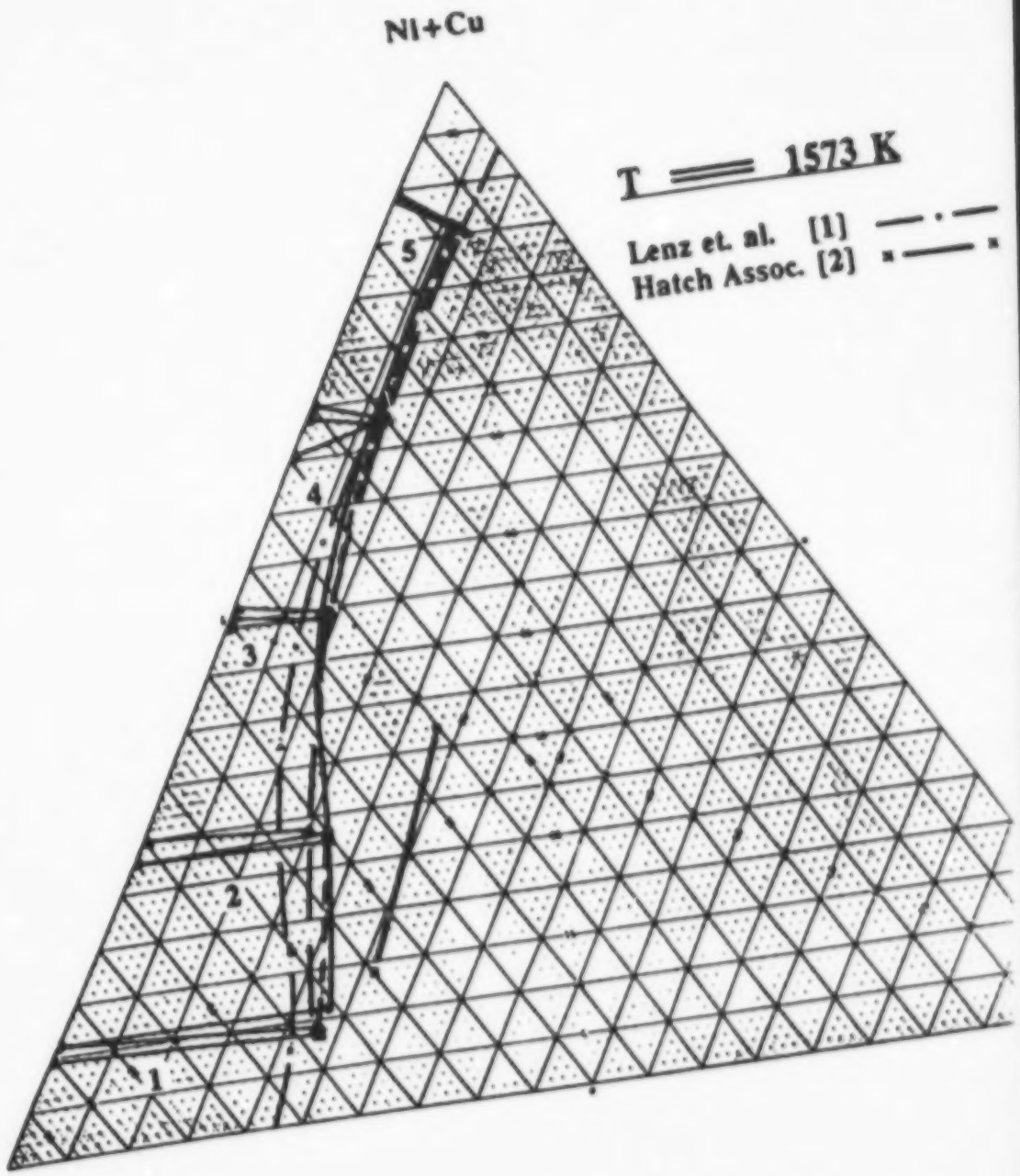

Figure 5: Representation of experimental results on a Fe-Ni+Cu-S pseudoternary syst

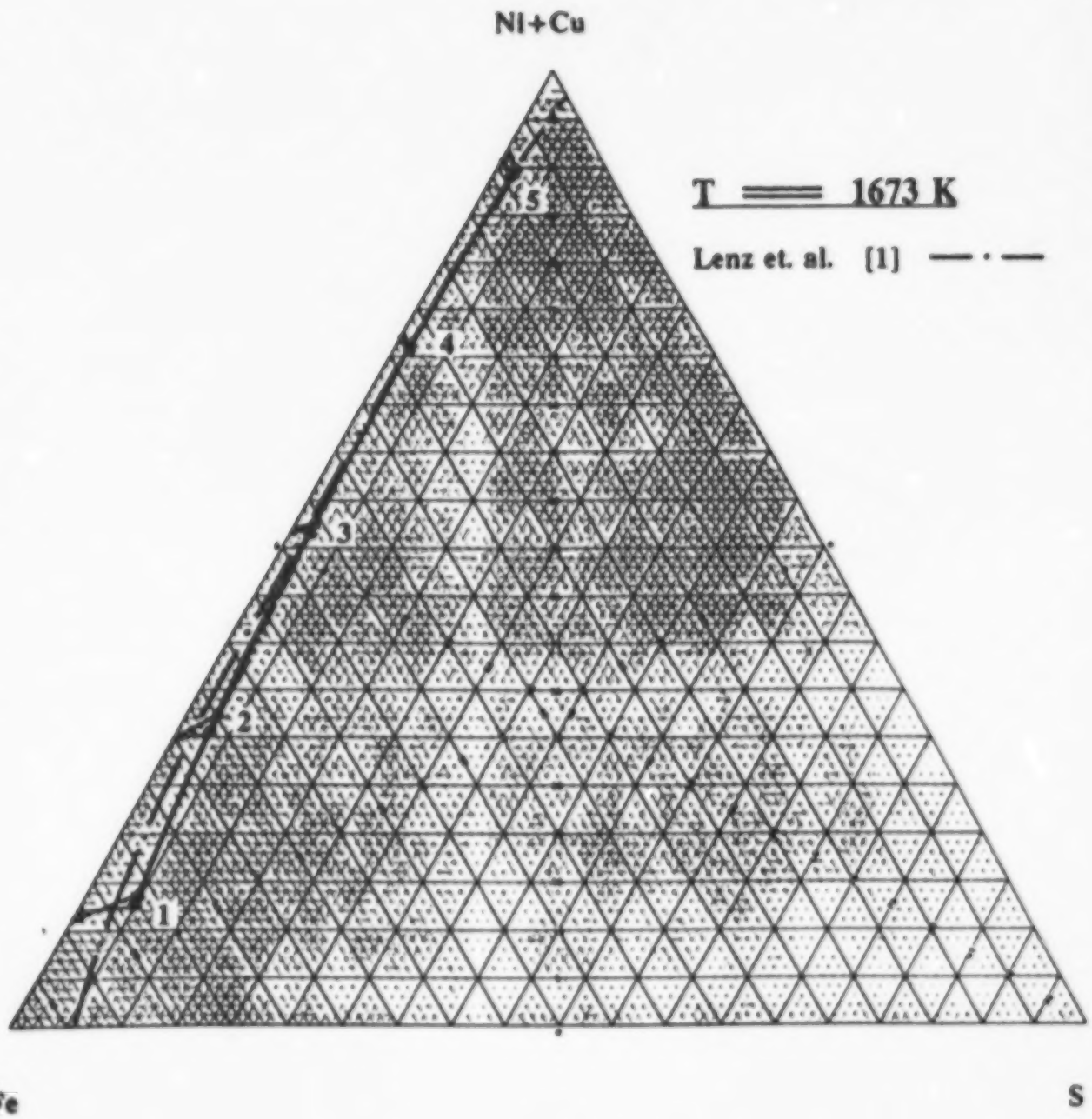

Figure 6: Representation of experimental results on a Fe-Ni+Cu-S pseudoternary system at 1673 K.

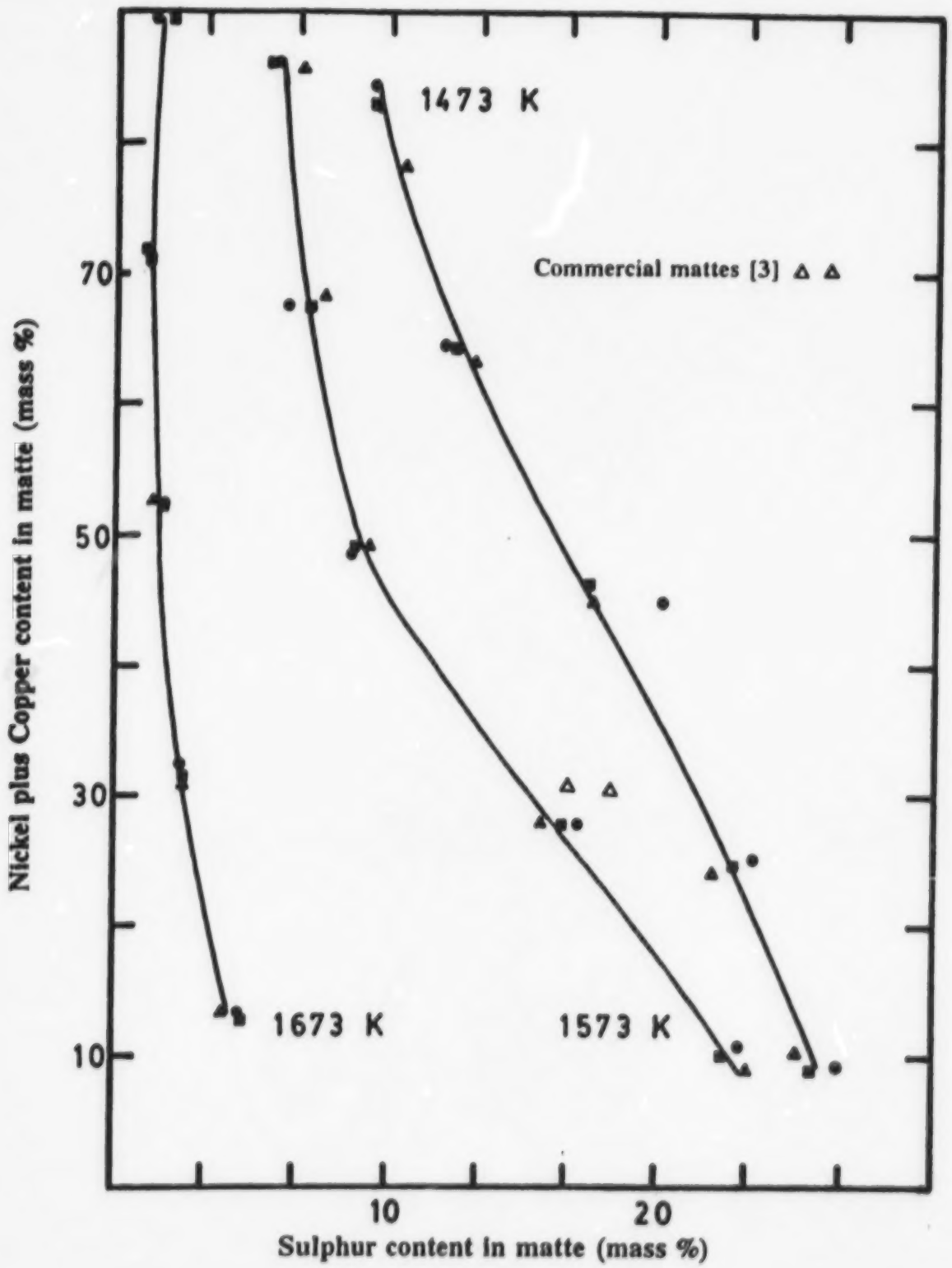

Figure 7: Effect of nickel plus copper on sulphur content in matte at different Ni:Cu ratio and temperatures.

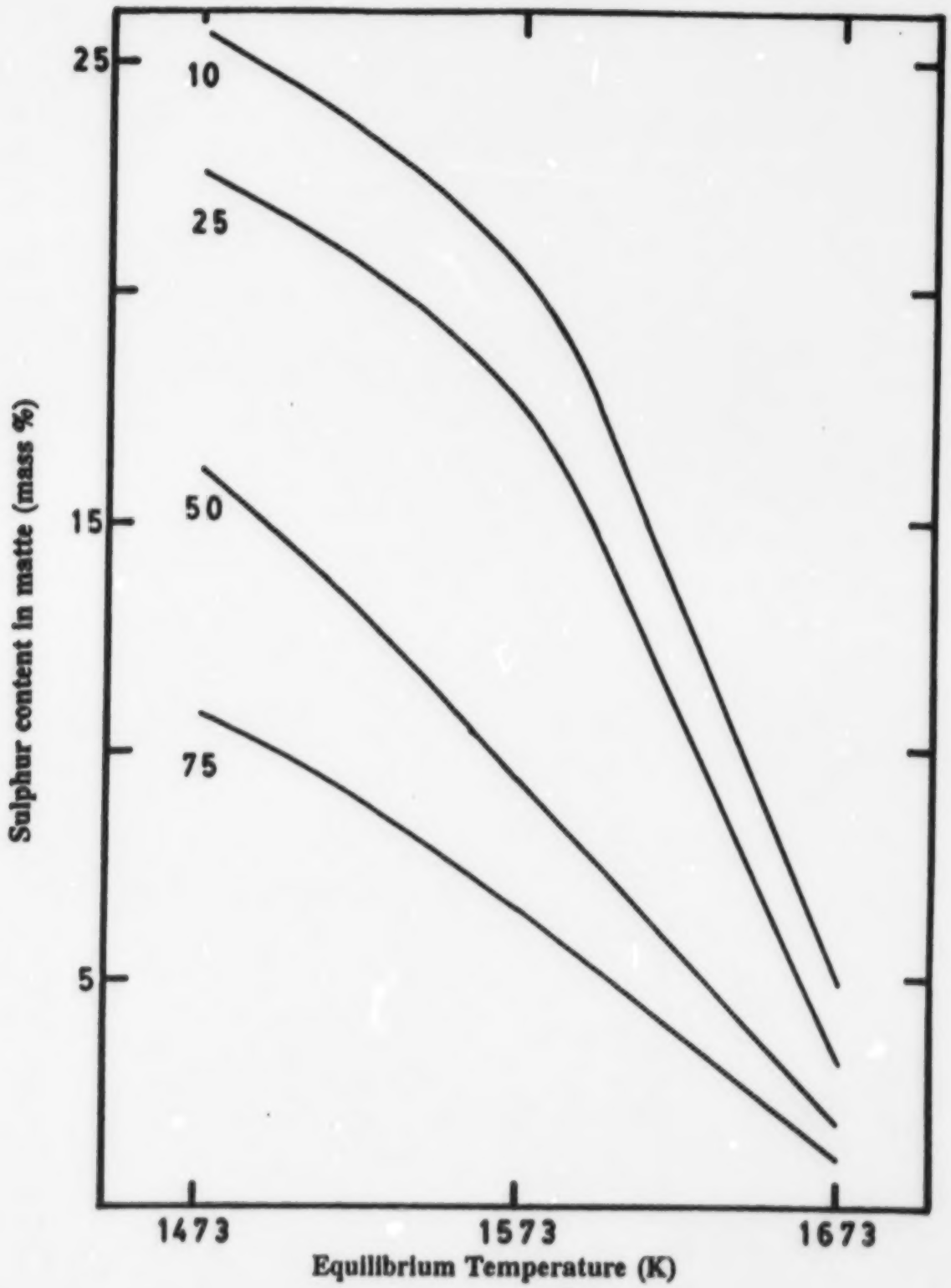

Figure 8: Relationship between the matte grade (Ni+Cu, denoted by the numbers below the curves) and its sulphur content at different temperatures.

Part III

Surface Tension and Wetting Behavior of Nickel Mattes

ABSTRACT

Surface tension and interfacial tension nickel matte is an important thermodynamic property which affects phenomena such as localized corrosion of refractories, infiltration of matte into refractories and entrainment of pay metal into slags. In this study, the surface tension of Ni-Fe-S matte was measured using the sessile drop technique together with a high temperature x-ray radiographic setup.

To obtain the profile coordinates required for surface tension calculation, a computer program was developed to digitize the drop profiles. This new digitization technique was found to be reliable and less time consuming. The surface tension data obtained for the Ni-Fe-S system showed an increase in Fe content in the matte corresponds to a decrease in surface tension. This decrease showed a negative deviation from the ideal rule of additivity.

INTRODUCTION

The *surface tension*, γ of a liquid can be defined as the change in free energy per unit change in area of the surface. Formally, this can be written as

$$\gamma = \left[\frac{dG}{dA}\right]_{T,P} \qquad (1)$$

To measure surface tension quantitatively at elevated temperature (above 1000 °C), the *sessile drop technique*, which is the technique employed in this study, is one of the limited few methods available. To perform a measurement using this technique, a drop of the liquid under investigation is put on a level solid surface and is allowed to come to thermal and

mechanical equilibrium. The shape of the resulting drop, is defined by the well known Laplace equation:

$$\Delta P = \gamma\left[\frac{1}{R_1} + \frac{1}{R_2}\right] \qquad (2)$$

The ΔP term ($\Delta P = \rho gh$) on the left refers to the pressure difference across any given point on the drop surface while the two $\frac{1}{R}$ term's on the right refer to the two principle radius of curvatures at the point under question. From the above equation, it can be seen that the surface tension can be obtained once the density and the shape of the drop is known. However, since the differential form of equation 2 cannot be solved analytically, surface tension has to be calculated through two means; a) by using the Bashforth and Adams table and b) by solving the equation numerically with the use of a computer.

THE SESSILE DROP TECHNIQUE

Recently, a computer procedure[1] developed for solving the Laplace equation became available. With this procedure, the surface tension of the liquid can be evaluated by providing the computer with the density of the liquid and a set of coordinate points (more than 20) on the drop profile. Besides the surface tension, the contact angle between the solid and the liquid is also calculated.

Previously, the coordinate points were obtained by firstly printing the drop image on photographic paper and then manually digitizing it with a

[1] Y. Rotenberg, L. Boruvka and A.W. Neumann, J. Colloid Inter. Sci.,93, (1983), pp169-83

routine is that it is both time consuming and susceptible to human bias.

To circumvent the shortcoming of manual digitizing, a computer program written in PASCAL was developed to digitize the drop profile. The program was designed based on the fact that if the photographic negative (figure 1a) of a drop image is back-illuminated by a light source, the light intensity profile across a line on the image will look something like figure 1b. At the edge of the drop, the light intensity suddenly drops from that of the drop to the background value. It is this abrupt change that allows the program to detect the edge and thus obtain points from the profile. Figure 2 shows the flow chart of the computer program. Prior to digitizing, the images to be digitized are converted into image files with the use of image acquisition software and hardware.

SURFACE TENSION EXPERIMENTS

Surface tension experiments were carried out using a high temperature x-ray radiographic setup shown in figure 3. The samples under study were encapsulated in quartz capsules to ensure that equilibrium condition is achieved. The capsule is leveled and then put into the furnace. Once the sample is at temperature, x-ray photographs are taken at different time intervals. These images are then processed later with the digitization program for surface tension evaluation. Different matte composition and substrate materials have been used. Substrate materials include alumina, quartz, sapphire and magnesia.

RESULTS

Surface tension calculations were performed on various systems using profile data obtained from both manual and computer assisted digitization,

the results are shown in figures 4, 5 and 6. Figure 4 represents data for gold as a function of temperature. Gold was chosen in the assessment study because of its purity and it is not prone to surface active elements such as oxygen. Figures 5 and 6 are results for a Ni-Fe-S matte plotted as a function of time under a constant atmosphere of $P_{S_2} = 10^{-2}$ atm.

From the results shown, it can be seen that the results obtained from both method are in very good agreement. Looking at the results for gold, the data obtained from this investigation are in very good agreement with literature data.

Using the new digitizing technique, the surface tension and contact angle of the Ni-Fe-S matte system were measured at 1200 $^{\circ}$C. The results are shown in figure 7 and 8. The surface tension of Ni-matte was found to decrease with increasing Fe content. The decrease in surface tension with Fe showed a negative deviation from the ideal rule of additivity. As shown in figure 8, contact angles decrease with increasing Fe content. Figure 8 also showed that Ni-matte wets alumina more readily than quartz.

SUMMARY

1. A computer assisted digitizing technique,based on the characteristic light intensity profile across the drop, is developed.

2. Data obtained from manual and computer digitizing were compared. The results indicated that computer digitization is a reliable method for generating profile data.

3. Surface tension and contact angle of Ni-matte on various substrates were measured. The surface tension and contact angle both decreases with increasing Fe content. The decrease in surface tension showed a negative deviation from the ideal rule of additivity.

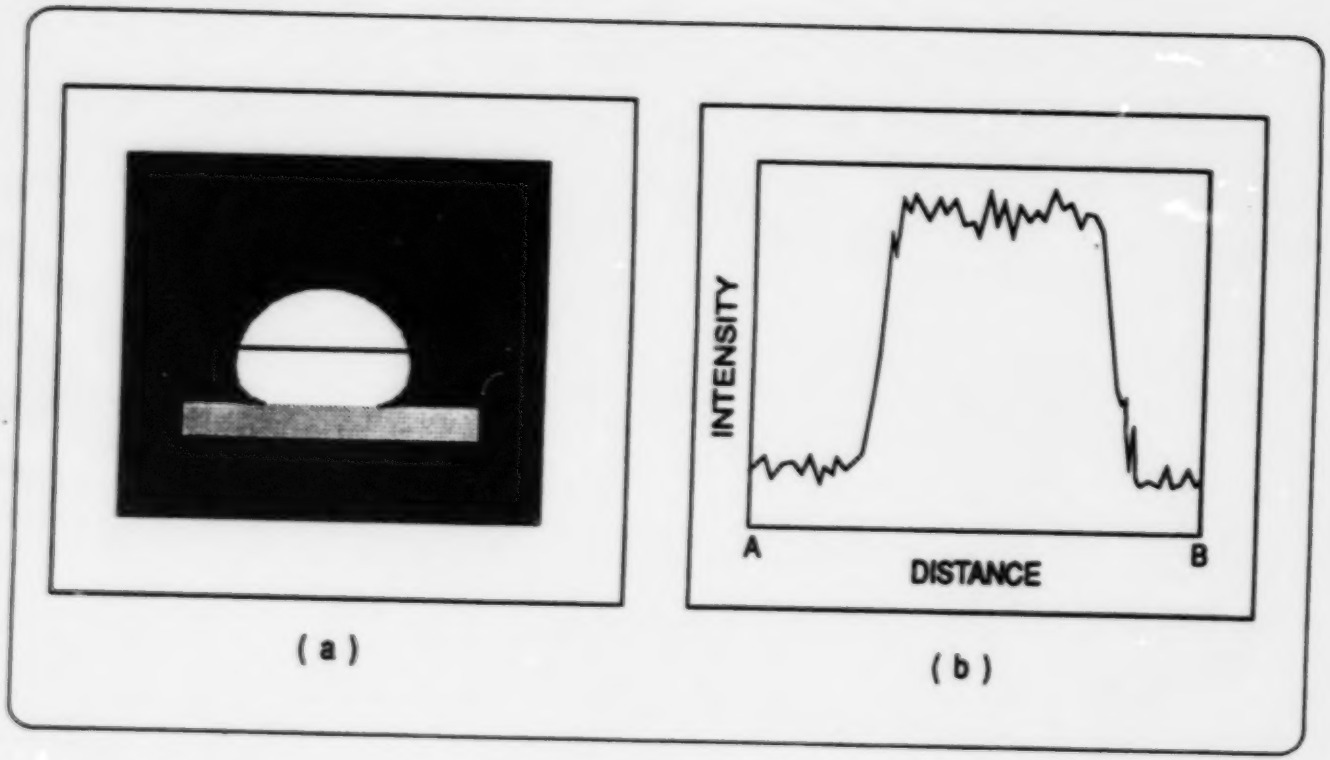

Figure 1. Schematic showing a) drop image on negative; and b) light intensity profile across line AB.

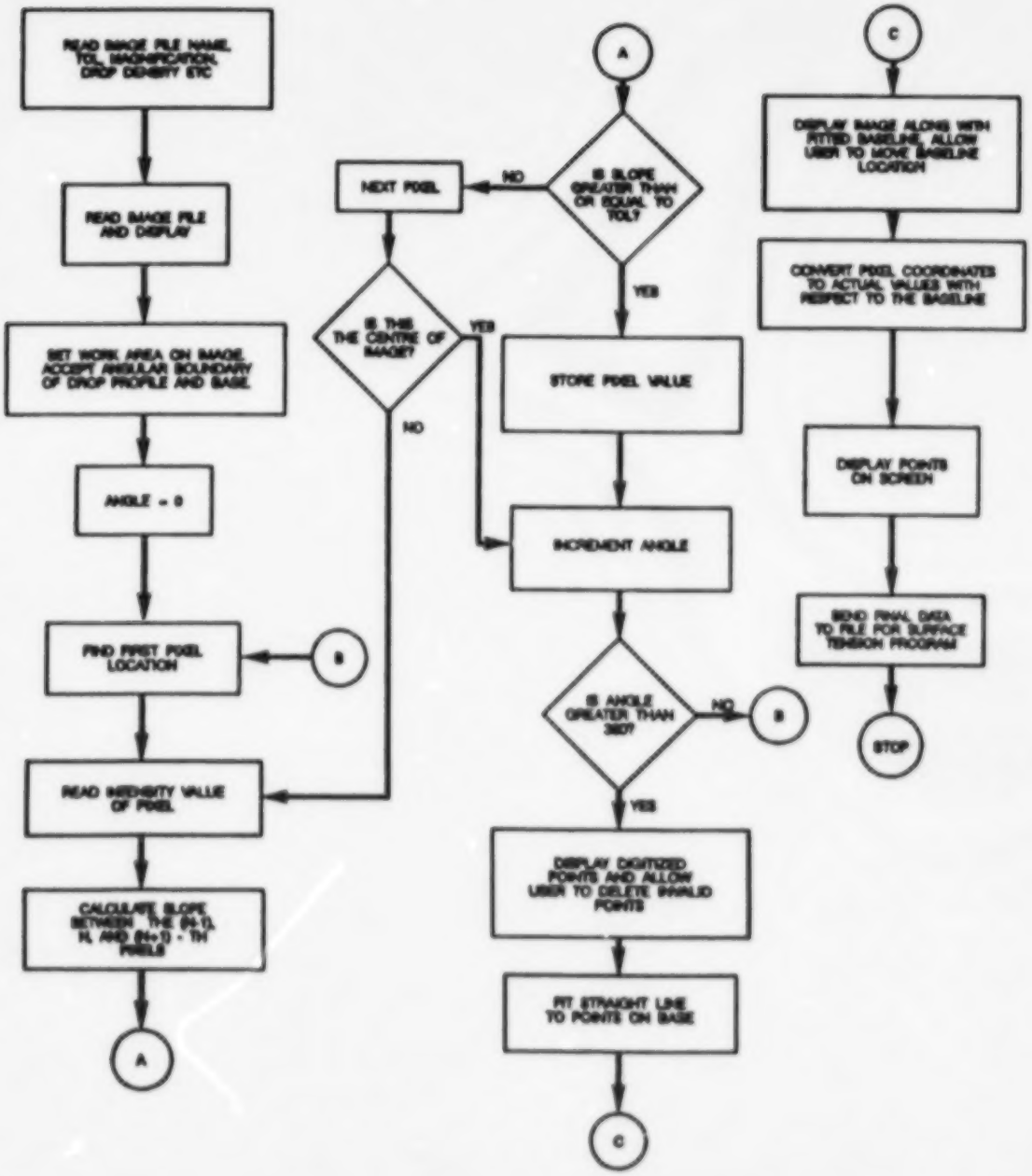
READ IMAGE FILE NAME, TOL, MAGNIFICATION, DROP DENSITY ETC
READ IMAGE FILE AND DISPLAY
SET WORK AREA ON IMAGE, ACCEPT ANGULAR BOUNDARY OF DROP PROFILE AND BASE
ANGLE = 0
FIND FIRST PIXEL LOCATION
B
READ INTENSITY VALUE OF PIXEL
CALCULATE SLOPE BETWEEN THE (N-1), N, AND (N+1) - TH PIXELS
A
A
IS SLOPE GREATER THAN OR EQUAL TO TOL?
NO
NEXT PIXEL
YES
IS THIS THE CENTRE OF IMAGE?
YES
NO
STORE PIXEL VALUE
INCREMENT ANGLE
IS ANGLE GREATER THAN 360?
NO
B
YES
DISPLAY DIGITIZED POINTS AND ALLOW USER TO DELETE INVALID POINTS
FIT STRAIGHT LINE TO POINTS ON BASE
C
C
DISPLAY IMAGE ALONG WITH FITTED BASELINE, ALLOW USER TO MOVE BASELINE LOCATION
CONVERT PIXEL COORDINATES TO ACTUAL VALUES WITH RESPECT TO THE BASELINE
DISPLAY POINTS ON SCREEN
SEND FINAL DATA TO FILE FOR SURFACE TENSION PROGRAM
STOP

Figure 2. Flowchart outlining the operation sequence of the drop digitization program.

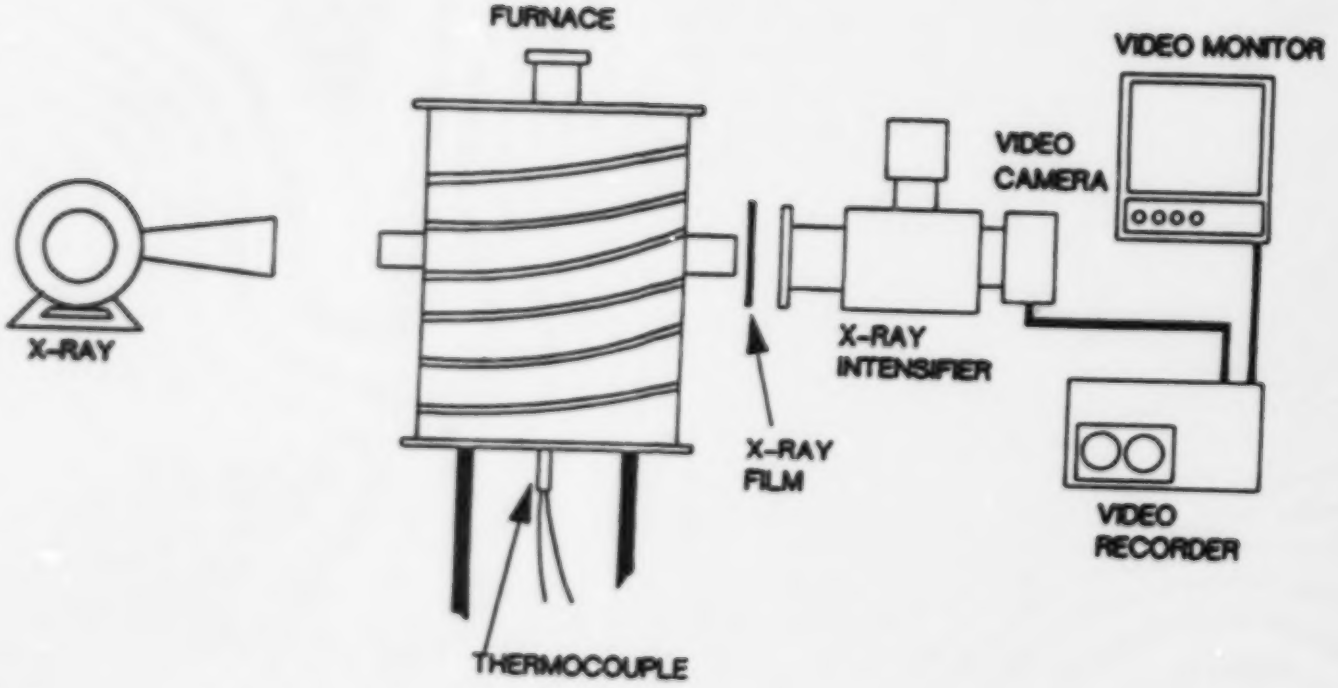

Figure 3. High temperature x-ray radiographic apparatus.

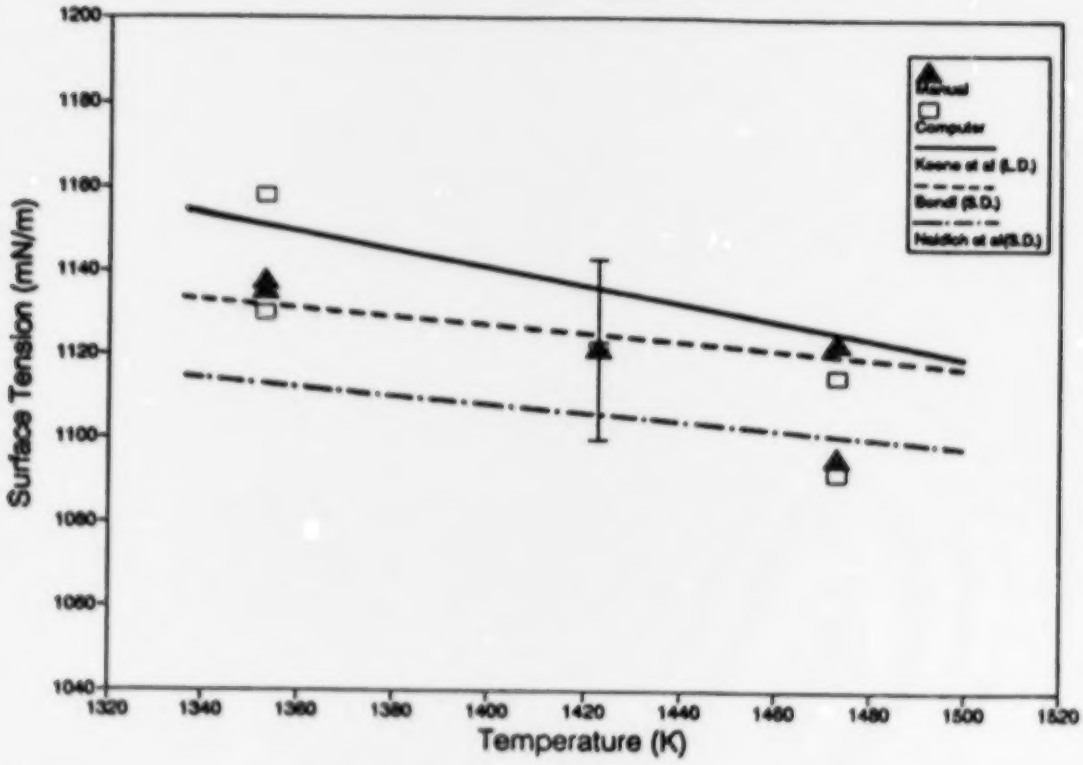

Figure 4. Surface tension of gold as a function of temperature. Error bar on centre represents a 2% deviation of that particular value.

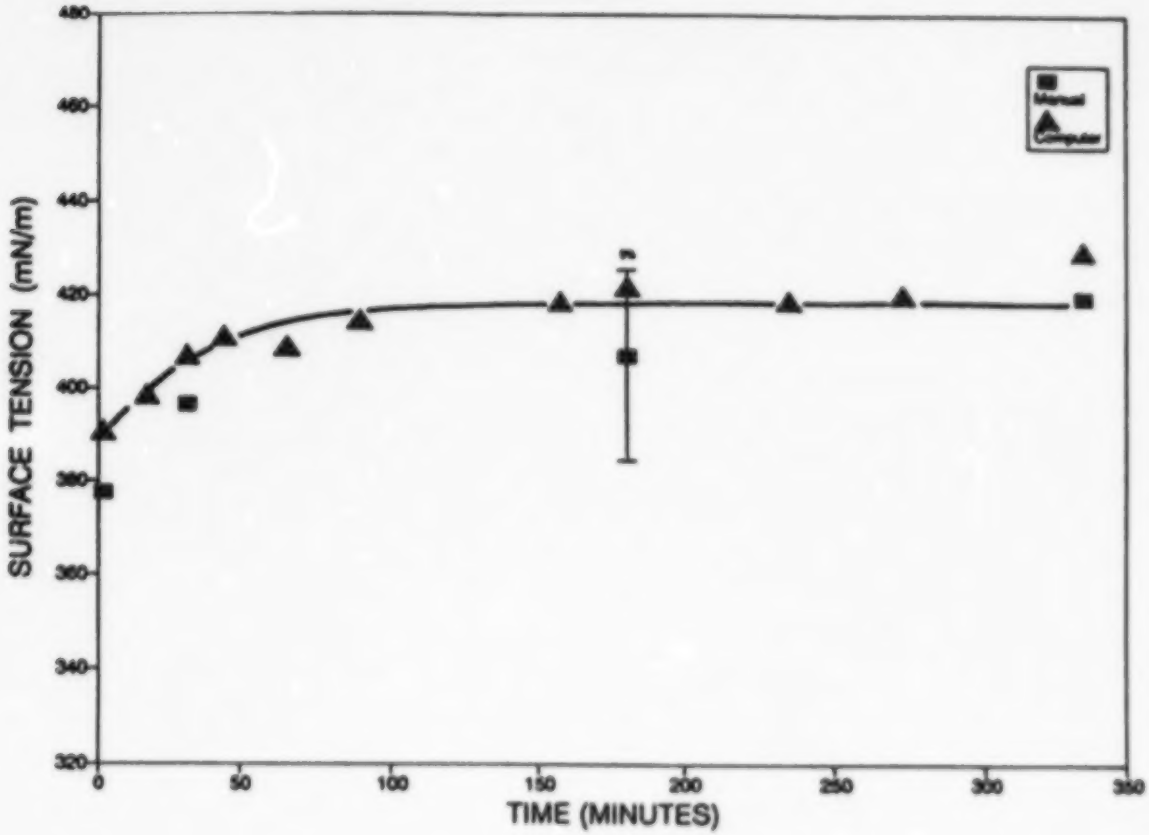

Figure 5. Time dependence of surface tension of a Ni-Fe-S matte measured at 1200 °C under a constant sulphur pressure of 10^{-2} atm.

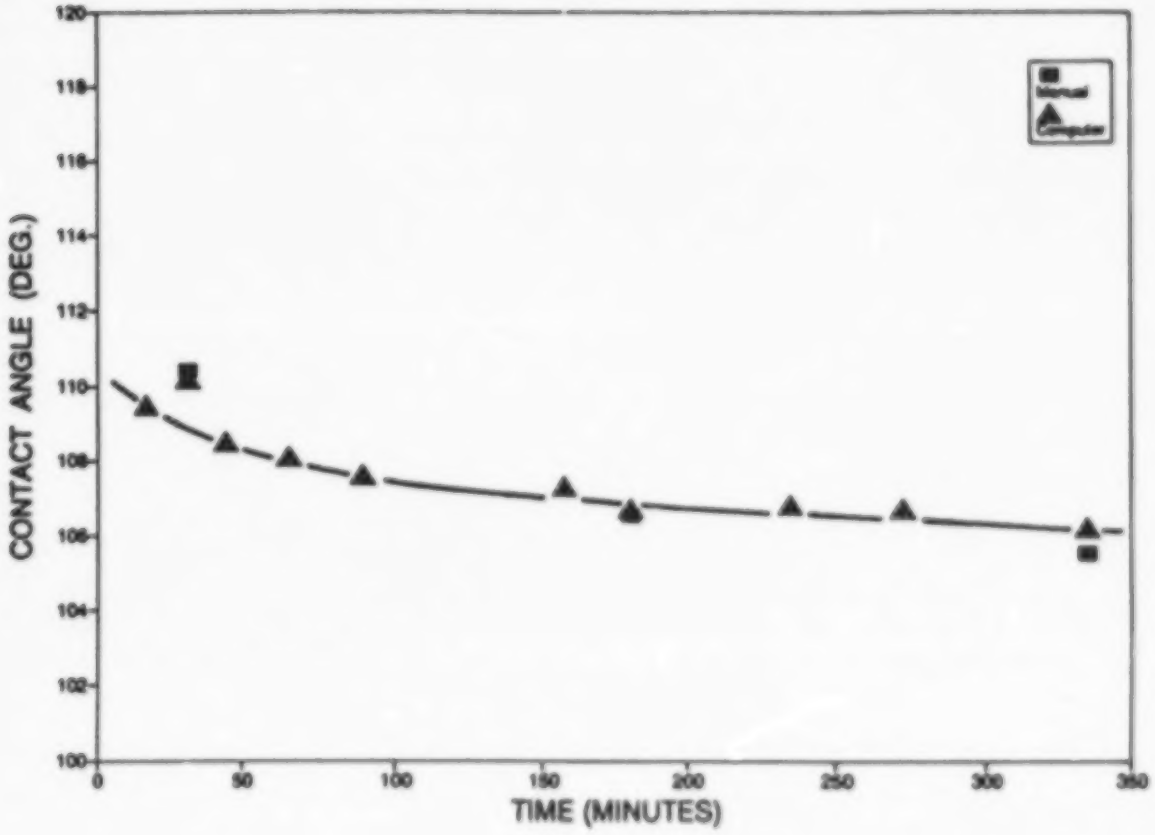

Figure 6. Contact angle of the matte in figure 5 as a function of time. The substrate material is alumina.

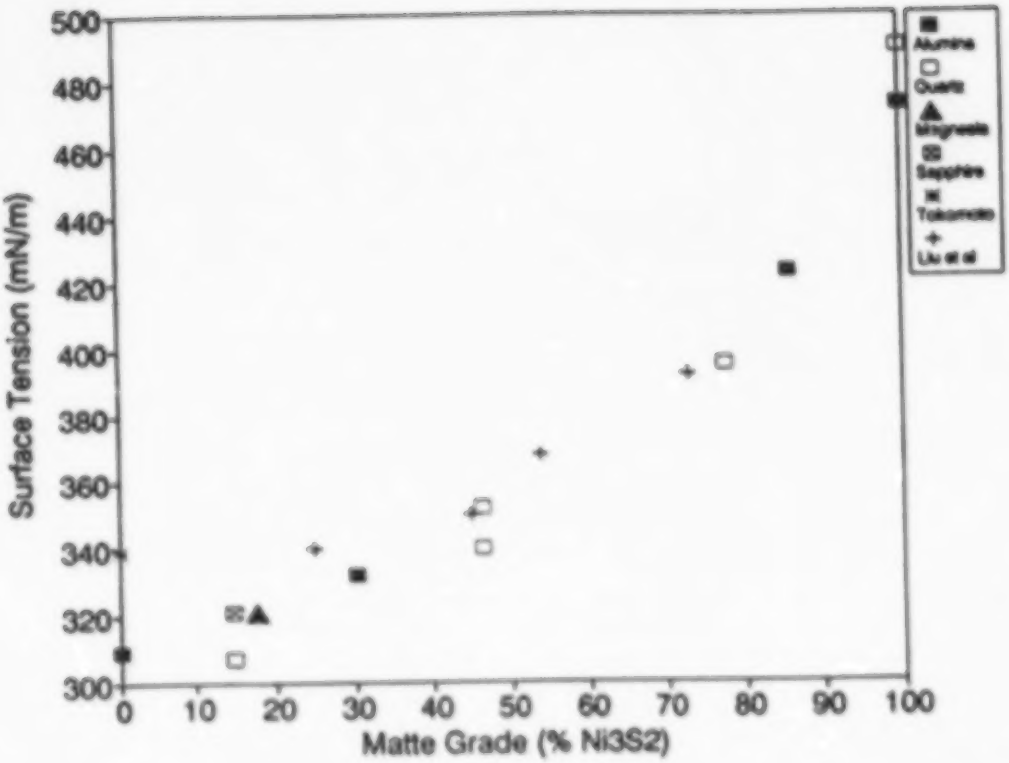

Figure 7. Surface tension of Ni-Fe-S matte as a function of matte composition. Temperature of measurement is 1200 °C.

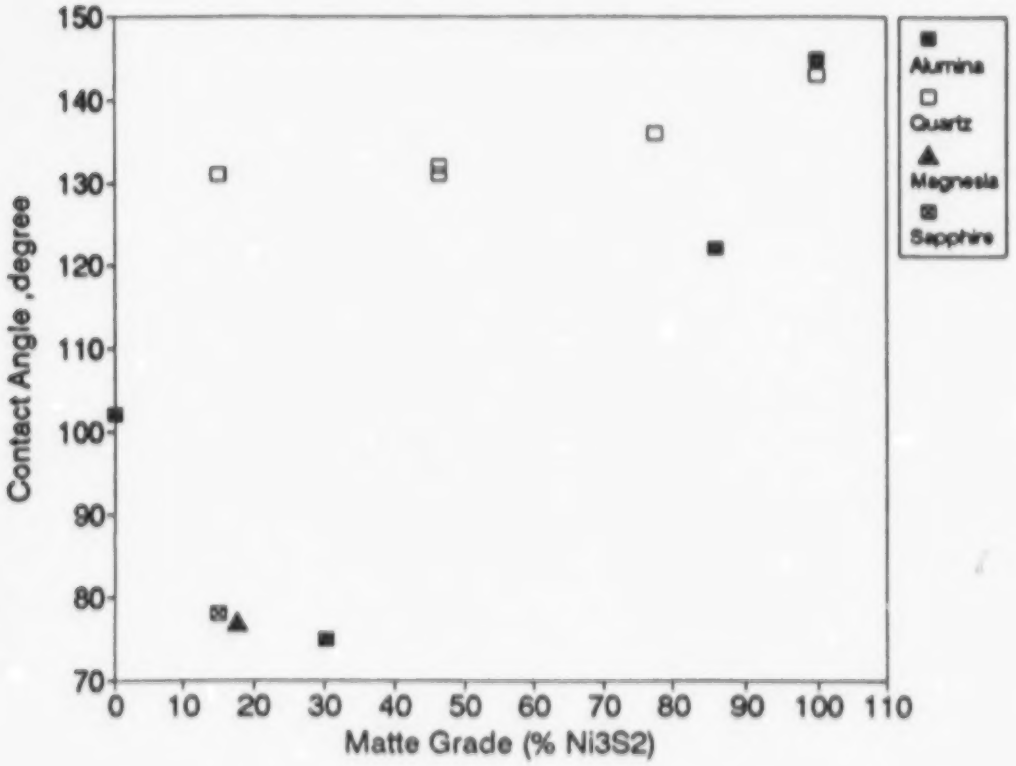

Figure 8. Contact angle of Ni-Fe-S matte on various substrate materials as a function of matte composition at 1200 °C.

Part IV

Oxygen Solubilities in Ni-Fe-S-O Melts

I. INTRODUCTION

Thermodynamic knowledge of the quaternary Ni-Fe-S-O system is necessary to gain a better understanding of nickel smelting and nickel matte converting. The oxygen in the matte is an important parameter since the aim of these extractive processes is to remove iron and sulphur by oxidation. While much data are available for the oxygen and sulphur solubilities in copper mattes, very little information exists on nickel mattes. Detailed reviews of the subsystems of the Ni-Fe-S-O system, including equilibrium studies and theoretical treatments of the literature data, are available [1-4], however, high temperature investigations of the quaternary system are lacking. Some data exist on

oxygen and sulphur solubilities in industrial nickel mattes [5,6] and copper-nickel mattes [7] in equilibrium with a slag phase.

The present study is confined to an investigation of the quarternary Ni-Fe-S-O system, in which liquid melt is in equilibrium with a gas phase, defined in terms of the four independent variables: temperature, partial pressure of oxygen, partial pressure of sulphur, and the Ni/(Ni+Fe) atomic ratio in the condensed phase. In addition, the conditions necessary for saturation of the nickel-iron sulphide melt with an oxide phase are investigated.

II. EXPERIMENTAL DESIGN

A. Apparatus

The furnace assembly is shown in Figure 1. A molybdenum resistance wound furnace was designed to accommodate a 100 mm constant temperature zone for equilibration of liquid matte and gas, in the temperature range, 1473 to 1573 K. The system was closed gas tight by flanges and end caps joined to the alumina furnace tube by compression 'O'-ring seals. An alumina crucible, 39 mm nominal i.d. and 89 mm in length, was contained in an alumina outer crucible. A push rod assembly introduced the crucible into the equilibration zone of the furnace at a controlled rate and also permitted rapid quenching of the sample.

In addition, the furnace assembly supported a quartz sampling tube (4.0 mm i.d.), alumina rod (6.0 mm i.d.) for introduction of the gas mixture and a type R thermocouple for temperature control. A ZrO_2-magnesia stabilized solid electrolyte electrochemical cell was used to monitor the approach to equilibrium. The crucible assembly was thermally insulated by a crucible lid and a series of alumina baffles.

B. Gas System

Liquid Ni-Fe-S-O melts were equilibrated with Ar-CO-CO_2-SO_2 gas mixtures such that the equilibrium partial pressures of oxygen and sulphur were in the ranges, $10^{-11.50}$ to $10^{-8.50}$ and $10^{-3.00}$ to $10^{-2.00}$ atmospheres, respectively. Each gas was stripped of moisture through contact with anhydrous calcium sulphate and phosphorous pentoxide. In addition, trace carbon dioxide was absorbed from the Ar and CO streams by ascarite, and the oxygen potential in the Ar stream was reduced to approximately 10^{-15} atmospheres by a copper getter furnace operating at 723 K.

Flow rates were determined by the use of capillary flow meters calibrated with a soap bubble flow tube. The line pressure for each gas was regulated by adjustable level bubblers containing n-butyl phthalate, which allowed long-term stability of gas flow rates.

Thorough gas mixing was achieved through a series of pyrex mixers designed to create turbulent flow into a mixing chamber. The gas mixture was then directed into a 3-L buffering ballast followed by introduction into the equilibration zone of the furnace. Gas leaving the furnace was stripped of sulphur dioxide in a packed column containing 10 percent aqueous sodium hydroxide solution, and the tail gas was directed to a CO burnoff.

The initial composition of Ar, CO, CO_2 and SO_2 gases required to produce a defined equilibrium (P_{O_2},P_{S_2}) at a specified temperature and total pressure was calculated using the FACT (Facility for the Analysis of Chemical Thermodynamics) System data base and programme available at McGill University, Montreal, Quebec. The gas compositions allowable are subject to thermodynamic constraints as well as the gas mixing ratios and upper and lower limits of flow rate tolerated by laboratory flow meters. Figure 2 shows the partial pressures of oxygen and sulphur allowable using CO-CO_2-SO_2 gas mixtures with an inert partial pressure of 0.3 atmospheres Ar and a

minimal initial partial pressure restriction of 0.005 atmospheres.

C. Electrochemical cell

The use of stabilized zirconia solid electrolytes to measure oxygen potentials in gaseous atmospheres and liquid melts is well covered in the recent literature [8,9].

The galvanic cell used in this investigation is described schematically as:

$$\underline{O}(\text{liq matte}),\ LaCrO_3,\ Pt \mid ZrO_2 + MgO \mid Pt,\ Fe/FeO$$

ZrO_2 (+5 wt% MgO) tubes closed at one end, with dimensions of 10 mm o.d, 7 mm i.d., and 100 mm length, were obtained from Nippon Kagaku Togyo Co. Ltd. Each tube was cut to 40 mm length and loaded with 0.5 mm diameter Pt lead wire coiled at one end and 2 grams of high purity (99.8%) iron powder. Good contact between the solid electrolyte and Pt wire was ensured by a spring-like design of the Pt coil and by compression with a piece of alumina rod (see Figure 3). Alumina powder, oven-dried at 120°C, followed by a layer of ceramic cement were used to seal the half cell. The lead contained in the Ni-Fe-S-O melt was constructed from 0.5 mm diameter Pt wire tightly wound about a $LaCrO_3$ rod, 2 mm in diameter and 10 mm in height. This lead assembly was contained in a 5 mm o.d. alumina sheath.

The overall electrochemical cell arrangement, shown in Figure 3, was such that the solid electrolyte tube and Pt-$LaCrO_3$ lead wire were immersed 8 mm below the surface of the Ni-Fe-S-O melt and were 5 mm apart. Emf readings were determined using a Leeds & Northrup Potentiometer (Model 7553-6) standardized with a 1.0185 V cell.

D. Experimental Procedure

A 50 gram sample of nickel matte (prepared from high purity Ni_3S_2, Fe_9S_{10} and Fe_2O_3) was loaded into an alumina crucible which was supported in the lower, cool end of the furnace tube. After thorough flushing of the furnace assembly with Ar, a $CO/CO_2/SO_2$ gas mixture of known P_{O_2} and P_{S_2} was introduced at a total gas flowrate of 150 ml/min. The crucible containing the sample was raised slowly into the hot region of the furnace by means of an outer crucible-push rod assembly. Once the crucible was positioned in the equilibration zone,

a solid electrolyte electrochemical cell was lowered into the melt sample and emf values were recorded as a function of time.

After a minimum of 24 hours, a 2 gram sample of melt was aspirated, allowed to air cool for a few seconds and then quenched in cold water. After sampling, the gas composition was changed and equilibration between melt and gas was resumed. This procedure was repeated for a total of six incremental increases in P_{O_2} for a single series at constant P_{S_2}.

E. Analysis of Matte Samples

Oxygen and sulphur contents in the melt samples were determined by a hydrogen reduction method similar to that employed by Kameda and Yazawa [10]. Dry hydrogen gas was introduced into a quartz chamber, which was heated to 1173 K and which contained a 30 x 10 mm alumina boat filled with matte, resting in an outer quartz sample holder. Oxygen in the sample reacted with hydrogen gas to form H_2O vapour which was adsorbed in the first of two weighing tubes containing phosphorous pentoxide. A third empty weighing tube was used to monitor atmospheric weight changes.

Sulphur also reacted with hydrogen and formed H_2S which was collected by bubbling the off gas into an Erlenmyer flask of absorbent solution. This solution was prepared from a 1-L aqueous solution of 10 g cadmium acetate ($(CH_3COO)_2Cd{\cdot}2H_2O$), 40 g zinc acetate ($(CH_3COO)_2Zn{\cdot}2H_2O$) and 30 ml glacial acetic acid.

The oxygen content in a sample was determined from weight gains in the weighing tubes; and the sulphur content was calculated from the additional weight loss of the sample.

A scanning electron microscope (Hitachi, Model S-570) equipped with an X-ray diffraction analyzer (Kevex Microanalyst 8000) was used to determine the metals content in the Ni matte samples. In addition, Al, Ni, Fe and S elemental maps were generated for polished cross-sections of the crucible-matte-oxide assembly.

III. RESULTS

A. Determination of Equilibration Times

The partial pressures of oxygen in the liquid melt were determined by substitution of Jacobsson and Rosen's [11] expression (Equation 1) for the reference P_{O_2} into the Nernst equation.

$$\log P_{O_2} = 5.518 - 27403/T + 0.377 \log T \quad (750\text{-}1580\ K) \qquad (1)$$

Their relation was selected since it is applicable in the temperature range of interest and it yielded values which are fairly representative of the literature.

As shown in Figure 4, emf values obtained from the solid electrolyte electrochemical cell decreased rapidly and then stabilized after 20 hours, during the first approach to equilibrium within a series of experiments. After 24 hours of equilibration, the gas composition was changed to a higher partial pressure of oxygen. The electrochemical cell responded accordingly and indicated that equilibrium had been established in an additional 20 hours. It was found that solid electrolyte failure occurred after 60 hours of exposure to liquid matte.

The partial pressures of oxygen based on gas mixing in the first and second experiments (Fig. 4) are 1.00×10^{-10} atmospheres and 3.16×10^{-10} atmospheres, respectively. The P_{O_2}'s, as determined by emf measurements, are 2.3×10^{-10} (0.1645 V) and 7.3×10^{-10} (0.2011 V) atmospheres, respectively. The precision associated with cell fabrication is $\pm$10% as demonstrated by replicate experiments in this study; however, this alone cannot account for the disparity between partial pressures of oxygen determined by gas mixing and by solid electrolyte measurements.

Experimental errors may arise from uncertainties in the determination of the cell temperature, in the measurement of the cell voltage or in the evaluation of the reference oxygen partial pressure. The most common source of intrinsic error to the material [12] is dependence of the fractional ionic and electronic conductivities upon temperature and ambient oxygen partial pressure. Magnesia-stabilized zirconia is present as a mixture of cubic and tetragonal zirconia, the cubic form being necessary for ionic conduction, at temperatures above 1400°C. Decomposition to tetragonal ZrO_2 and MgO occurs below this temperature followed by the martensitic

tetragonal-monoclinic transformation at 1240°C. MgO-stabilized ZrO_2 may be effective as an oxygen ion conductor below these temperatures since phase composition is dependent on thermal history [13]. An electrolyte that has been treated at a temperature above 1400°C, to ensure that it contains a high fraction of cubic zirconia, will only gradually lose its cubic structure with time.

In cell fabrication, it is important that good contact exists between the Pt lead wire and $LaCrO_3$ cermet rod and between the other lead wire and reference electrode. In addition, impurities such as SiO_2 in ZrO_2 and Ca in $LaCrO_3$ may lead to chemical reactions between the solid electrolyte and matte and to varying resistivities, respectively.

Nonetheless, in this study, solid electrolyte electrochemical cells proved to be very responsive to changes in partial pressures of oxygen and were instrumental in determining equilibration times.

Preliminary experiments in which samples of melt were chemically analyzed during equilibration of matte with gas were also conducted. Figure 5 shows how oxygen and sulphur contents vary with time for nickel mattes (atomic Ni/(Ni+Fe) = 0.50) approaching equilibrium with a gas mixture of composition, $10^{-9.00}$ atmospheres oxygen and $10^{-2.00}$ atmospheres sulphur, at 1473 K. Different initial concentrations of oxygen and sulphur were studied; however, in each case, equilibrium was achieved within 24 hours. The emf measurements, reported earlier, confirm that this length of time establishes equilibrium. Effort was made to prepare matte charges which were within 1 mass percent of the equilibrium oxygen and sulphur concentrations, to further ensure equilibrium states.

B. Oxygen Solubility Studies

1. Effect of P_{O_2}

Oxygen contents in Ni-Fe-S-O melts equilibrated with gas mixtures were found to increase with increasing partial pressure of oxygen up to a maximum value at oxide saturation. In Figure 6, mattes within the composition range, $0.19 < Ni/(Ni+Fe) < 0.79$, reach oxide saturation between $10^{-9.00}$ and $10^{-8.70}$ atm as indicated by their respective maxima. The onset of oxide saturation was determined using both increasing Ni/(Ni+Fe)

ratio in the matte phase and a change in the relationship between oxygen solubility and P_{O_2}, as criteria. With the occurrence of oxide formation, the Ni/(Ni+Fe) ratio in the matte phase must change, in accordance with the phase rule, to the composition defined by the temperature and partial pressures of oxygen and sulphur.

The dashed lines of Figure 6 represent three phase states at varying partial pressures of oxygen. The numbers in brackets indicate the Ni/(Ni+Fe) ratios in the matte phase. Oxygen solubility decreased as iron was oxidized from the matte phase or as the Ni/(Ni+Fe) ratio in the matte increased.

2. Effect of Ni/Fe Ratio

It is apparent from Figure 6 that oxygen contents in Ni-Fe-S-O melts are greater at lower Ni/(Ni+Fe) ratios. This effect is more clearly illustrated in Figure 7 which is a plot of oxygen content against Ni/(Ni+Fe) ratio for oxide-unsaturated mattes equilibrated with partial pressures of oxygen in the range, $10^{-10.00}$ to $10^{-9.00}$ atm. At constant P_{O_2}, oxygen content increases as the nickel to iron ratio decreases, presumably to a maximum solubility at oxide-saturation. Included in this figure are the oxide-saturated data of this study, corresponding to $P_{S_2}=10^{-2.00}$ atm, and Grimsey's [5] estimated upper limits of oxygen solubility, corresponding to magnetite-SO_2 saturation, for industrial nickel mattes.

3. Effect of Temperature

The oxygen solubilities in oxide-unsaturated Ni mattes equilibrated at 1473, 1523 and 1573 K are plotted against the logarithm of the partial pressure of oxygen in Figure 8. The data represent Ni mattes of the composition, Ni/(Ni+Fe) = 0.47, which were equilibrated with a partial pressure of sulphur of $10^{-2.00}$ atm. It is clear that the oxygen content in these mattes decreased as temperature increased, under the same set of experimental conditions.

C. Determination of Free Energy of Oxygen Dissolution

The equilibrium constant for reaction (2), the dissolution of oxygen in Ni mattes of various compositions,

$$1/2\ O_2(g) = \underline{O}(\text{Ni matte}) \qquad (2)$$

is given by

$$K = \frac{a_O}{P_{O_2}^{1/2}} = \frac{\%\underline{O}/100 \cdot f_O}{P_{O_2}^{1/2}} \qquad (3)$$

where a_O is the activity of oxygen, f_O is the activity coefficient of oxygen and the standard state for dissolved oxygen is 1 mass% solute in accordance with Henry's law for dilute solutions. Apparent equilibrium constants, K', may be experimentally determined from the oxygen solubilities and partial pressures of oxygen:

$$K' = \frac{\%\underline{O}/100}{P_{O_2}^{1/2}} \qquad (4)$$

Since the value of f_O approaches unity as the oxygen concentration approaches zero, it is possible to determine K from the y-intercept of the plot of the logarithm of the apparent equilibrium constant against oxygen concentration. Data for Ni mattes of various compositions: Ni/(Ni+Fe) = 0.44, 0.47 and 0.50; and temperature: T = 1473, 1523 and 1573 K were compiled from experimental values and from interpolation of Figure 7, and are presented in Figure 9.

It was assumed that the linear dependence of f_O on composition, shown in Figure 9, predominated also in the lower %O concentration range, where data are not available. Back extrapolation of the curves in Figure 9 corresponding to Ni/(Ni+Fe) = 0.47 at three different temperatures: 1473, 1523 and 1573 K; yielded K values which were substituted into Equation (5). The correlation coefficients of the curves which were fitted by linear regression are indicated in Figure 9 and ranged from 0.968 to 0.996.

$$\Delta G^\circ = -RT \ln K \qquad (5)$$

An expression for the standard Gibbs energy of oxygen dissolution in liquid mattes of composition, Ni/(Ni+Fe) = 0.47, in which $P_{O_2} = 10^{-2.0}$ atm was calculated,

$$\Delta G^\circ = -202.5 + 0.0660T\ (K)\ (\pm 1.5 kJ/mol) \qquad (6)$$

The accuracy of this method for determining free energies of oxygen dissolution is dependent on: (1) the lower limit of oxygen detection, which in these experiments was approximately 0.15%, and (2) the validity

of the assumption that f_O varies linearly with %O concentration as %O approaches zero.

IV. CONCLUSIONS

1. Oxygen solubilities were measured in Ni-Fe-S-O melts under the following conditions: $10^{-11.50} \leq P_{S_2} \leq 10^{-8.50}$ atm; $10^{-3.00} \leq P_{S_2} \leq 10^{-2.00}$ atm; $0.19 \leq$ Ni/(Ni+Fe) atomic ratio ≤ 0.85; and 1473 K $\leq T \leq$ 1573 K; using an experimental technique which involved equilibration between synthetic matte and $CO/CO_2/SO_2$ gases. Oxygen and sulphur contents range from less than 0.15 to 4.18 mass percent and 17.13 to 30.88 mass percent, respectively, in the oxide-unsaturated nickel-iron sulphide melts of this study.

2. Oxygen solubilities in Ni mattes increase with the equilibrium partial pressure of oxygen up to a maximum value at oxide-saturation.

3. The effect of an increased equilibrium partial pressure of sulphur is decreased oxygen solubility and increased sulphur solubility. Both oxygen and sulphur dissolution studies indicate that more oxidizing conditions are required to reach oxide saturation when the system is in equilibrium with higher P_{S_2}'s.

4. Oxygen solubility decreases as the Ni/(Ni+Fe) ratio in the matte phase increases. It is apparent that the ferrous metals content favours oxygen dissolution, in the form of Fe-O associations.

5. The oxygen content in oxide-unsaturated Ni-Fe-S-O melts decreases with temperature when all other variables are held constant. Oxygen solubility is enhanced by approximately 0.5 mass percent from 1573 K to 1473 K, over the range of P_{S_2}'s studied and at a metals content of Ni/(Ni+Fe) = 0.47.

6. The standard Gibbs' energies of oxygen dissolution in nickel-iron sulphide melts of the composition, Ni/(Ni+Fe) = 0.47, in which $P_{S_2} = 10^{-2.00}$ atm, are -104.4, -103.6 and -97.8 (±1.5 kJ/mol) at 1473 K, 1523 K and 1573 K, respectively. An expression for the temperature dependence of ΔG° in these liquid mattes is,

$$\Delta G^\circ = -202.5 + 0.0660\ T \quad (\pm 1.5\ \text{kJ/mol}).$$

In the composition range, $0.44 \leq Ni/(Ni+Fe) \leq 0.50$, oxygen solubility is enhanced in mattes of greater iron content as indicated by more negative values in ΔG^0.

7. SEM-EDS, x-ray diffraction and chemical analysis indicated that the oxide-saturating phase in equilibrium with Ni-Fe-S-O melts under the experimental conditions of this study, is a form of the nickel-iron spinel,

$$(NiO)_x \cdot (FeO)_{1-x} \cdot Fe_2O_3$$

in which the mass percent nickel is less than 2. It may be concluded that oxygen solubility in oxide-saturated Ni mattes decreases with increasing matte grade and is fairly independent of the partial pressures of oxygen and sulphur, within the ranges of the variables investigated.

REFERENCES

1. R.S. Celmer, "The Distribution of Minor Elements in Nickel Matte Smelting", University of Toronto, Ph.D. Thesis, 1987.
2. K.C. Hsieh and Y.A. Chang, "A Solid-State Emf Study of Ternary Ni-S-O, Fe-S-O, and Quaternary Fe-Ni-S-O", Metall. Trans. B., 17B, March, 1986, pp. 133 - 146.
3. F. Sehnalek and I. Imris, "Advances in Extractive Metallurgy and Refining", M.J. Jones, ed., The Institution of Mining and Metallurgy, London, 1972, pp. 39 - 62.
4. K.S. Yoshiki-Gravelsins, "The Thermodynamic Properties of Ni-Fe-S-O Melts", University of Toronto, Ph.D. Thesis, 1988.
5. E.J. Grimsey, "Oxygen in matte and oxidic nickel in slag", Proc. Australas. Inst. Min. Metall., 275, Sept. 1980, pp. 53 - 57.
6. J.M. Floyd, D.S. Conochie and N.C. Grave, "Measurement of Oxygen Potential in Slags in a Nickel Smelter Using Disposable-tip EMF Cells", Proc. Australas. Inst. Min. Metall., 270, June, 1979, pp. 15 -23.
7. N.I. Chalkina and B.P. Nedvetskii, "Forms of Oxygen Content in Copper-Nickel Mattes", Sov. J. Non-

Ferrous Met., 19, No. II, Nov., 1978, pp. 40 - 41.

8. N. Kamori, Y. Shibata and M. Tomono, "Measurements of Oxygen Pressure in a Copper Flash Smelting Furnace by an EMF Method", Metall. Trans. B., 17B, Mar., 1986, pp. 111 - 117.

9. M. Sasabe, K. Kobayashi, M. Tate, Y. Kuwano and K. Suzuki, "A Direct Measurement of Oxygen Partial Pressure in a Testing Blast Furnace", Solid State Ionics 3/4, North-Holland Publishing Company, 1981, pp. 575 - 579.

10. M. Kameda and A. Yazawa, "Effects of Partial Pressures of Oxygen and Sulphur on the Oxygen Content in Copper Matte", Studies in Metallurgy, Tohoku Univ., Sendai, Japan, 1969, pp. 159 -166.

11. E. Jacobsson and E. Rosen, "Thermodynamic Studies of High Temperature Equilibria 25. Solid state emf studies of the systems Fe-FeO, Ni-NiO and Co-CoO in the temperature range 1000 -1600 K", Scand. J. Metall., 10, 1981, pp. 39 - 43.

12. A-M. Anthony, J.F. Baumard and J. Corish, "Results of a Collaborative Study on Zirconia-Based Oxygen Gauges", Pure and App. Chem., 56, No. 8, 1984, pp. 1069 - 1094.

13. M. van Wijngaarden, J. Geldenhuis and R. Dippenaar, "MgO-Stabilized Zirconia Electrolytes", Iron and Steelmaker, Iron and Steel Society, April, 1988, pp. 35 - 44.

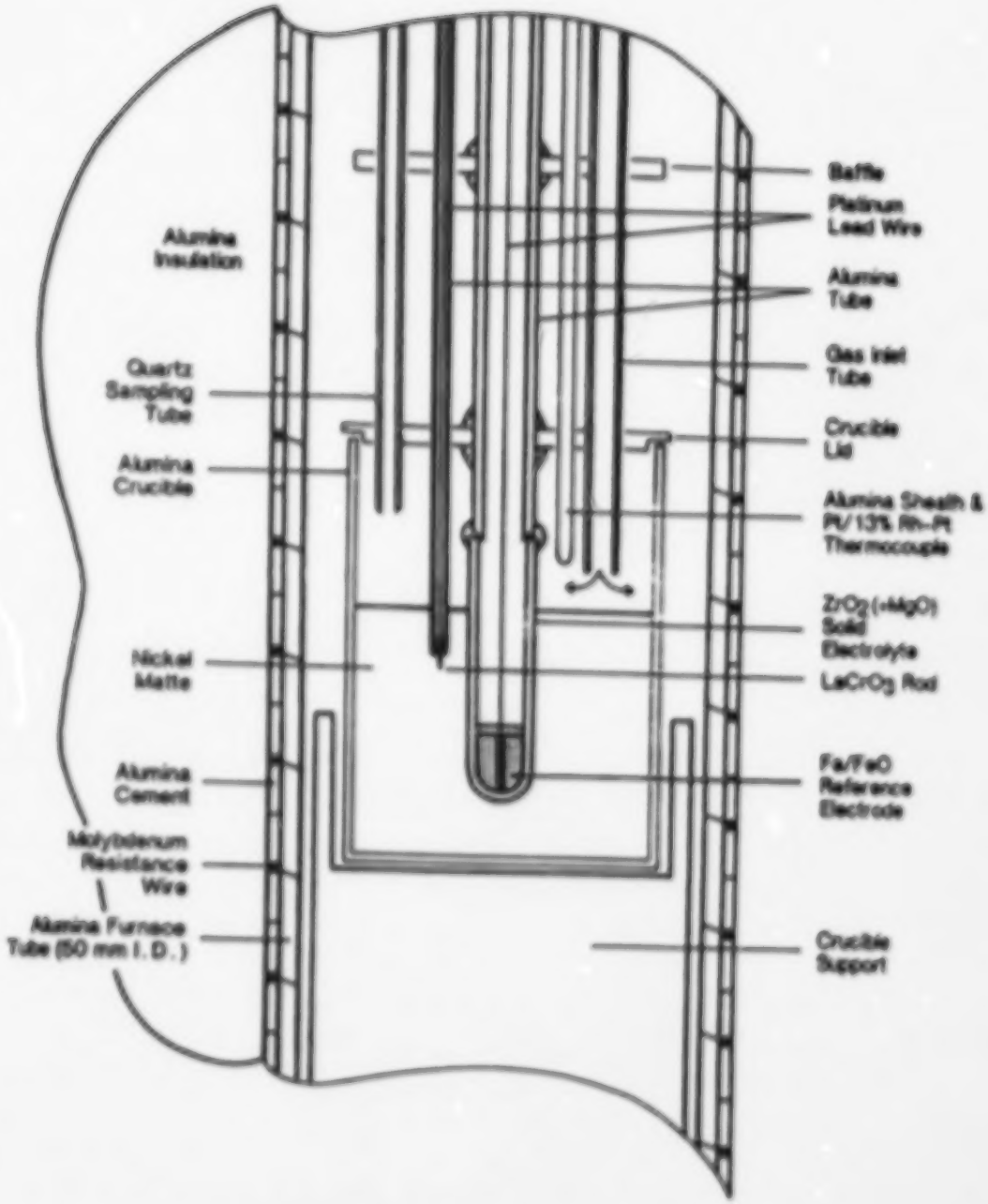

Figure 1 Experimental Cell

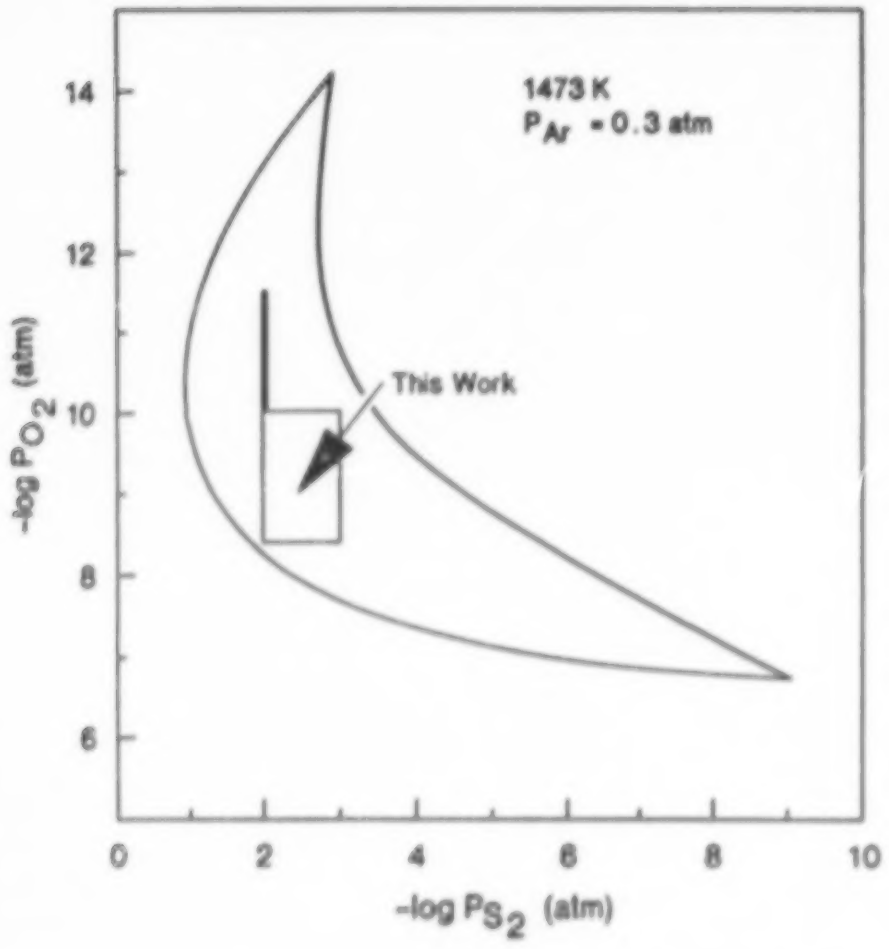

Figure 2 Ranges of oxygen and sulphur pressures available using $CO/CO_2/SO_2$ gas mixtures

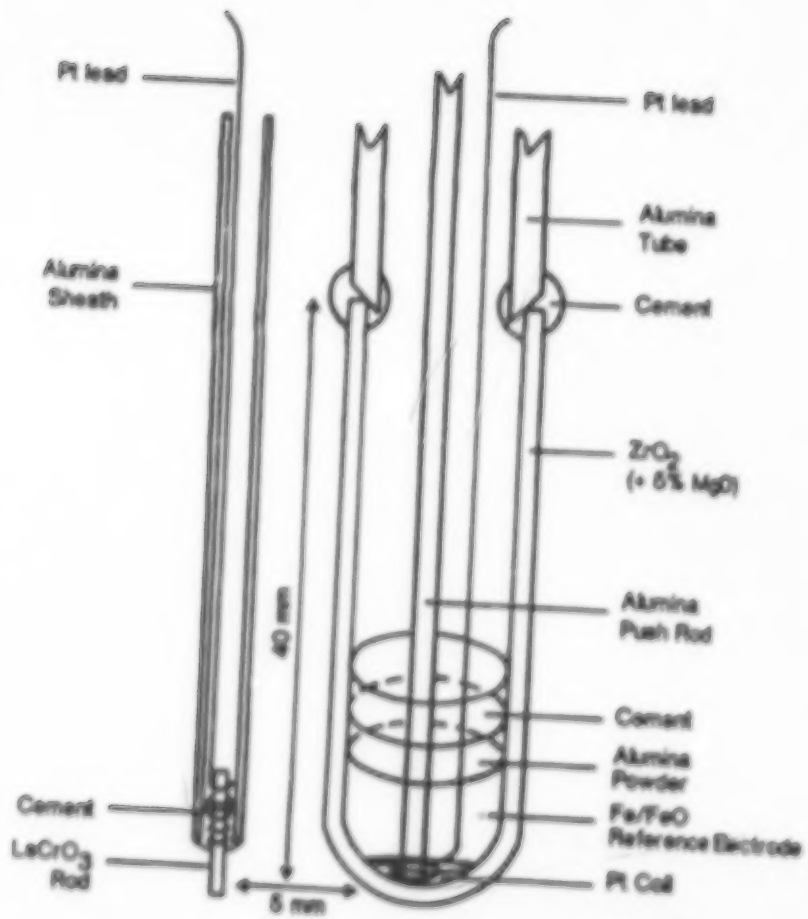

Figure 3 Electrochemical Cell

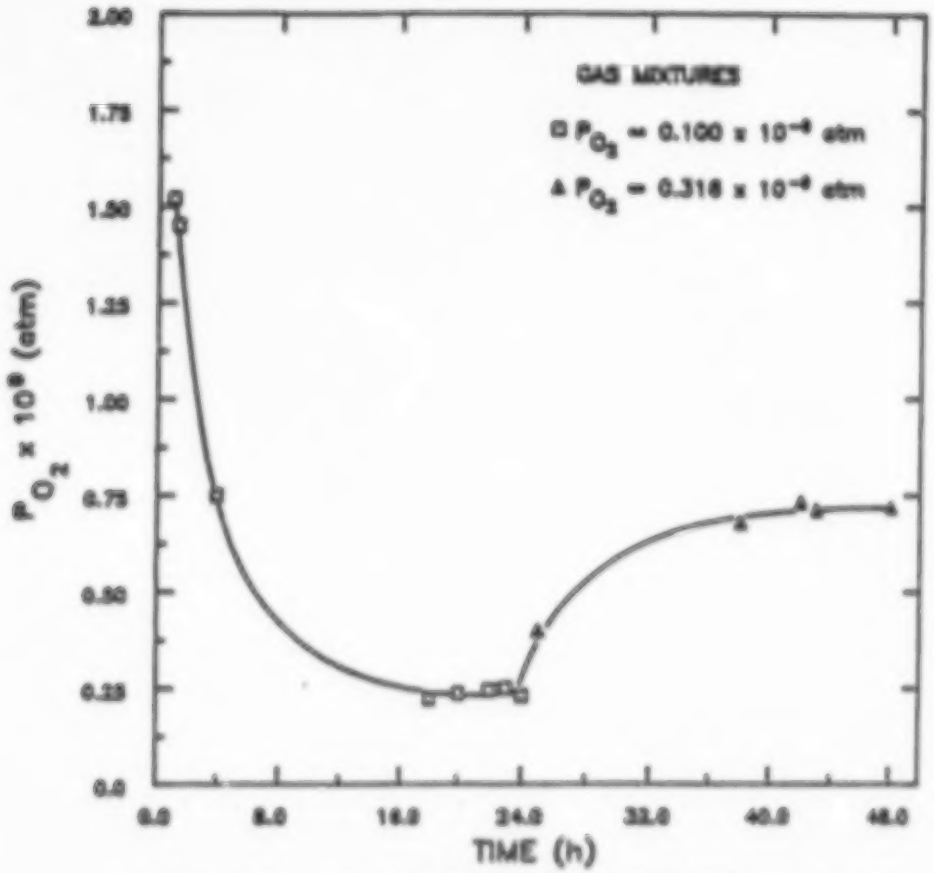

Figure 4 P_{O_2} Determined by EMF Measurements vs Time

$PO_2 = 10^{-9.00}$atm, $PS_2 = 10^{-2.00}$atm, T = 1473 K

(composition of gas mixture changed after t=24 h)

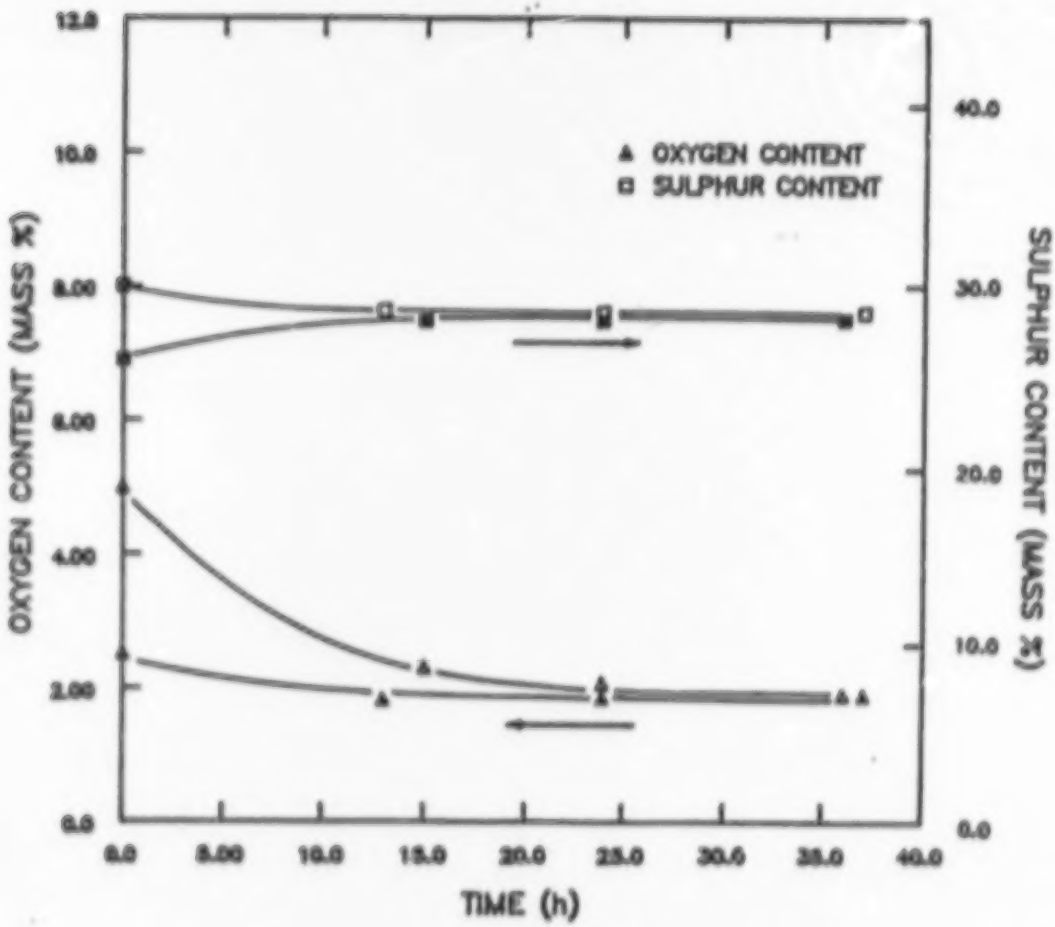

Figure 6 Oxygen and sulphur contents in Ni-Fe-S-O melts versus time

$P_{O_2} = 10^{-9.00}$ atm, $P_{S_2} = 10^{-2.00}$ atm, T = 1473 K

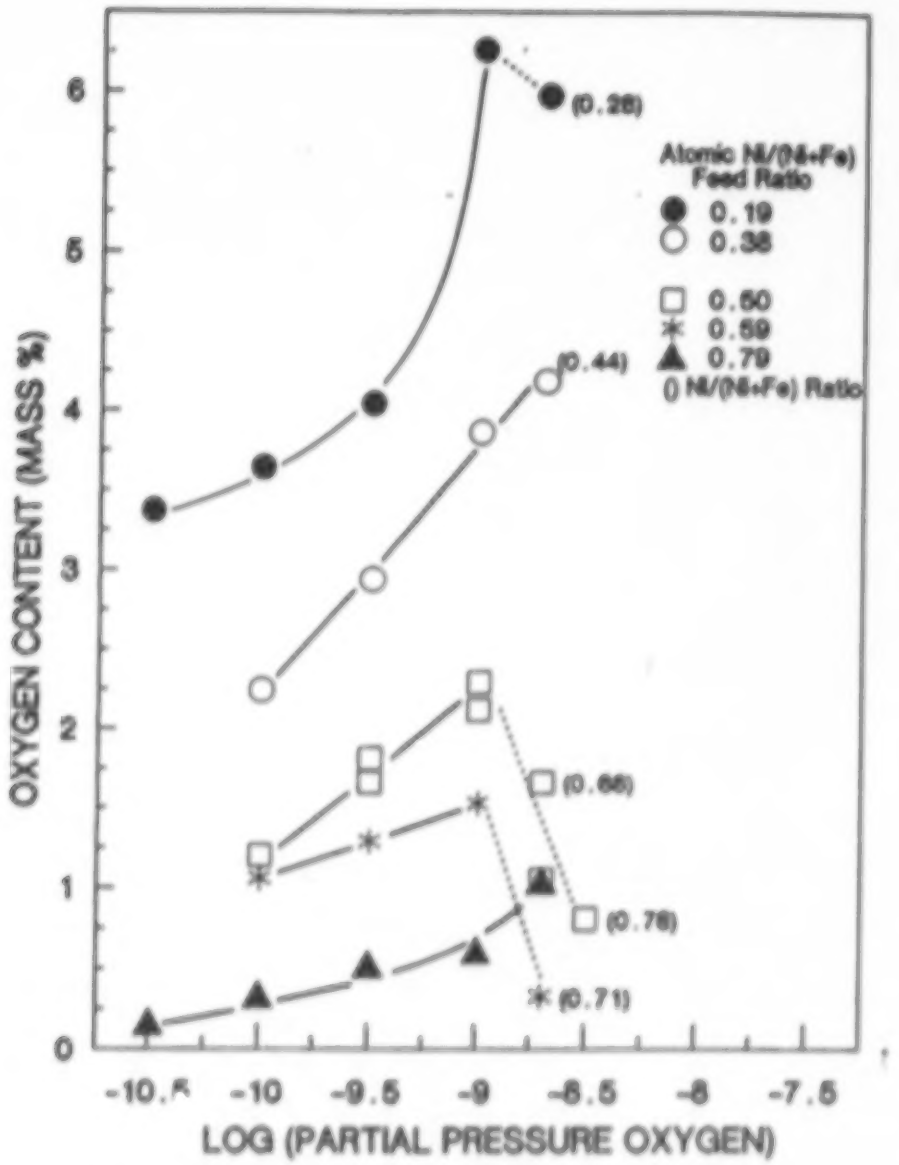

Figure 6 Oxygen Content versus Partial Pressure Oxygen
$P_{S_2} = 10^{-2.0}$ atm, $T = 1473$ K
— unsaturated ···· oxide-saturated

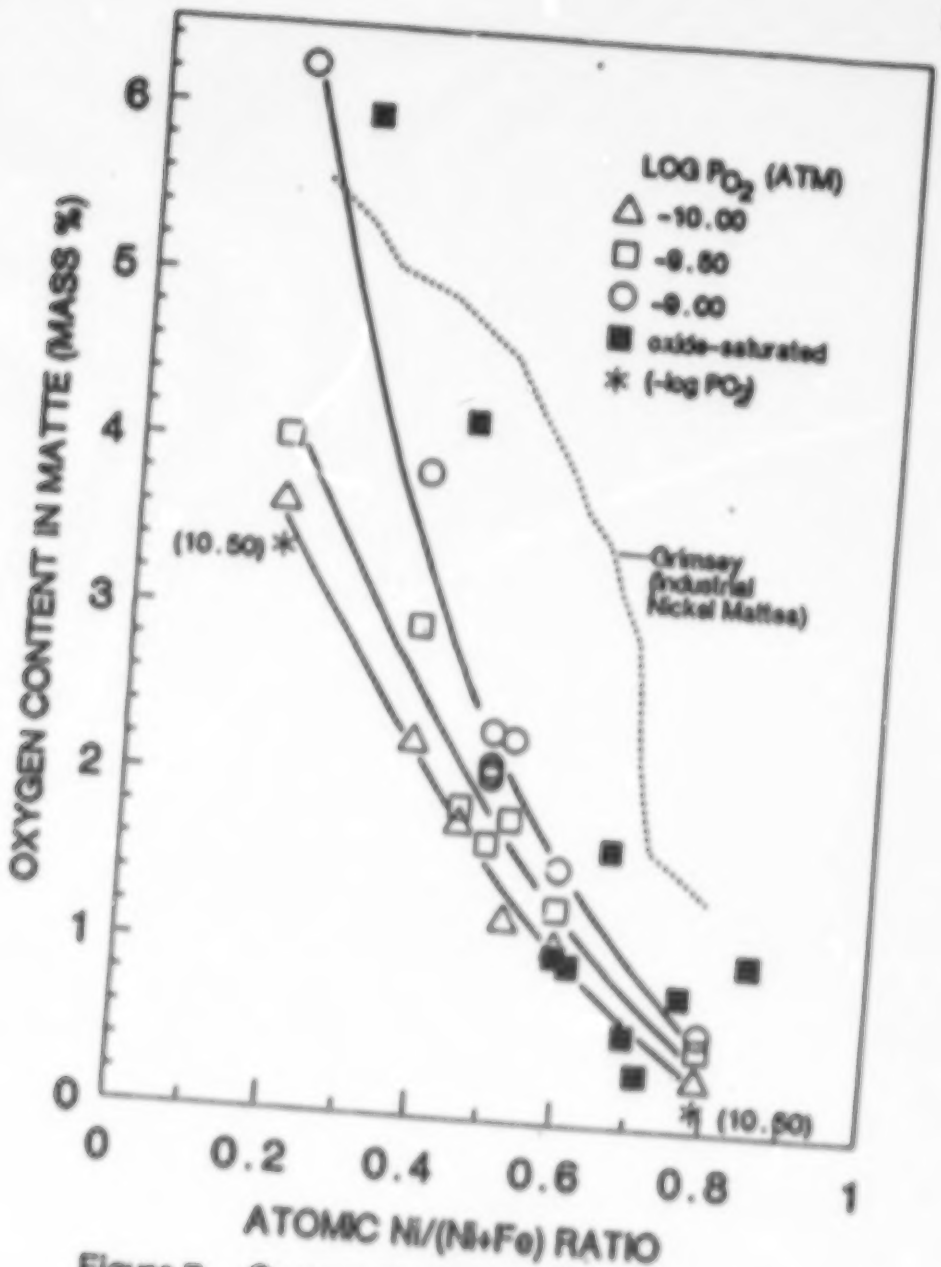

Figure 7 Oxygen Contents in Matte-Gas and Matte-Oxide-Gas Systems
(Matte-Gas Data: $P_{S_2} = 10^{-2.6}$ atm, T = 1473 K
Matte-Oxide-Gas Data: corrected for changing Ni/(Ni+Fe) Ratio)

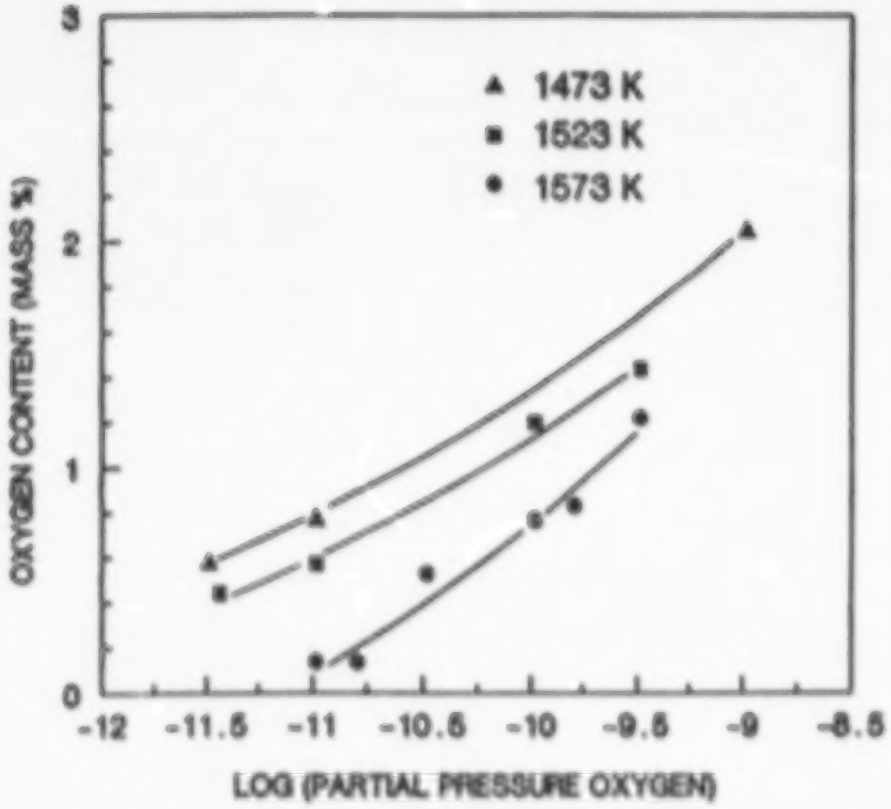

Figure 8 Oxygen contents in oxide-unsaturated Ni matte as a function of temperature Ni/(Ni+Fe)=0.47, $PS_2=10^{-2.0}$atm

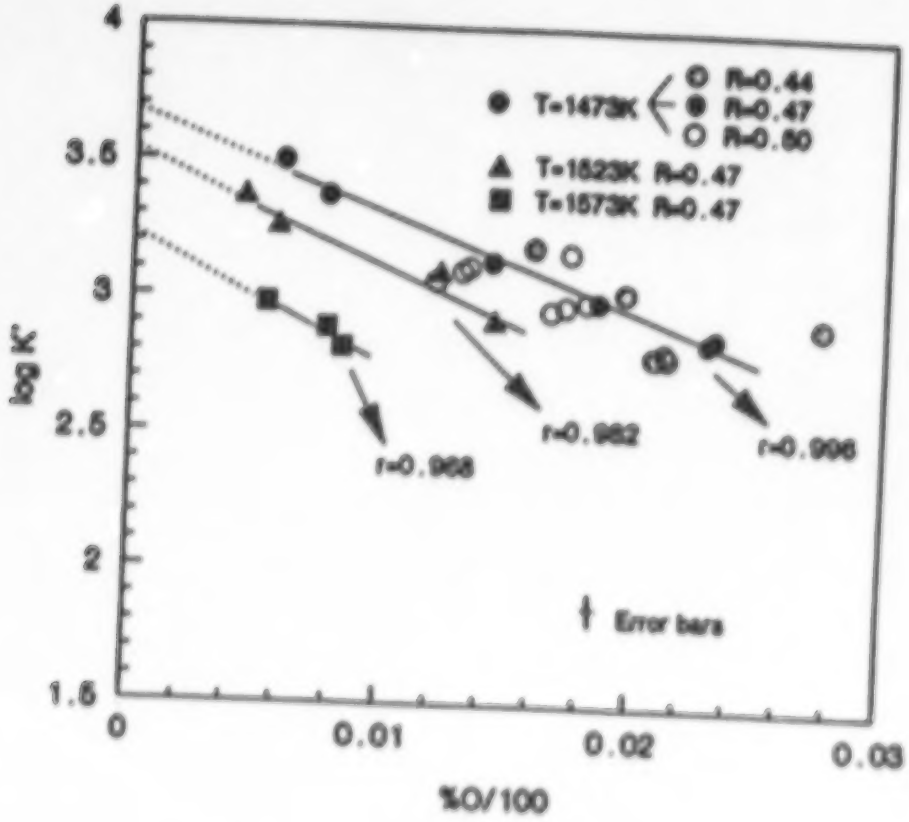

Figure 9 Logarithm of K', ($K'=[\%O/100]/P_{O_2}^{1/2}$), plotted against the mass fraction of oxygen. (Ni=Atomic Ni/(Ni+Fe) ratio, r=correlation coefficient)